ORIGINAL PAPER

Multi-vulnerability analysis for seismic risk management in historic city centres: an application to the historic city centre of La Serena, Chile

Pilar Baquedano-Juliá[1] · Tiago Miguel Ferreira[2] · Camilo Arriagada-Luco[3] · Cristián Sandoval[4] · Nuria Chiara Palazzi[5,6,7] · Daniel V. Oliveira[1]

Abstract

A comprehensive understanding of the elements at risk, through the identification of the main hazards, level of exposure and different dimensions of the vulnerability of the communities, is an essential step toward the definition and adoption of more effective risk reduction strategies. Historic urban centres have received special attention in the assessment of damage and physical vulnerability to earthquakes, but it is well known that vulnerability also depends on the social and demographic characteristics of communities. This paper discusses the application of a holistic approach aimed at assessing the seismic vulnerability of historic urban centres by considering their physical and social dimensions. Two index-based methodologies are presented, and the data are analyzed using the CENSUS block as the unit of study, which is scarcely present in the literature. The results of both indices are crossed through a matrix, which allows the classification of the blocks in five levels of priority and are mapped using a Geographic Information System tool. The Historic city centre of La Serena, one of the oldest in Chile, was selected as a case study. This historic city centre still preserves historic buildings of raw earth of diverse architectural typologies widely distributed throughout the country, which makes it relevant, not only by itself but as a model that can be replicated and extrapolated to other historic centres of similar constructive characteristics.

Keywords Historic city centres · Masonry buildings · Seismic vulnerability · Social vulnerability · Vulnerability index method

1 Introduction

Disaster risk is usually understood as the potential loss of life, injury or destruction or damage to assets that can occur to a system, society, or community in a specific period, determined probabilistically as a function of hazard, exposure, vulnerability, and capacity (UNISDR 2009). Historic centres have characteristics that make them particularly vulnerable to disasters. The constructive characteristics of buildings and the urban morphology in which they are inserted increase the fragility of their historic fabric and

---

their vulnerability to natural and anthropogenic hazards. The main underlying causes of their increasing vulnerability are climate change, population growth, lack of appropriate policies and regulations, and urbanization and poverty, especially in developing countries and Latin American urban centres (Bosher et al. 2019; Bruquetas Callejo et al. 2005; Carrión 2001; Rojas 2004).

At the global level, emphasis has been placed on the need to develop disaster risk and vulnerability indicator systems—integrating different dimensions of vulnerability, capacities, exposure of people and assets, hazard characteristics and the environment—to provide information to decision-makers on how to assess the impact of disasters on social, economic and environmental conditions (UN 2005, 2015). There has been a paradigm shift in the study of disaster-resilience of societies, from the focus on the study of the frequency and magnitude of threats and their quantification toward the consideration and evaluation of the vulnerability of societies through the identification, evaluation and classification of different dimensions of vulnerabilities and recovery capacities (Birkmann 2013).

Assessing vulnerabilities at the urban scale can be a resource-intensive task. Index-based methodologies are one of the analysis tools that have seen more significant development over the last years in this field. Their main advantage is that these tools offer a simple, cost-effective and time-efficient alternative, which makes them particularly attractive for risk analysis in developing countries, where economic and skilled human resources for heritage protection are limited or often non-existent.

Current studies addressing the seismic risk assessment of historic urban areas focus mainly on the analysis of physical vulnerability (Baquedano Juliá and Ferreira 2021). These methodologies have proven to be effective for the definition of risk mitigation strategies, such as the application of standardized structural strengthening devices (Ferreira et al. 2017a) or the management of the emergency phase through the proposal of evacuation routes (Anglade et al. 2020).

However, it is known that seismic vulnerability results not only from the interaction of physical and built environment systems but also from the social and demographic characteristics of each community. The concept of social vulnerability in disaster management was introduced in the 1970s when vulnerability involving socio-economic variables was recognized (Flanagan et al. 2011). Measures of social vulnerability acknowledge the combination of social, cultural, economic, political, and institutional processes that shape socio-economic differences in exposure and coping capacities to natural disasters.

Social vulnerability refers to the socio-economic and demographic factors that affect the risks and resilience of communities, in line with disaster evidence that shows that socially vulnerable people are more affected by death, property damage and housing damage. Different categories of people living in disaster-affected areas are not equally affected. As widely documented in the literature, the poorer tend to be significantly more vulnerable at all stages of the disaster cycle, i.e., before, during and after the event. Vulnerability to hazards is influenced by different social factors, including age, ethnicity, gender, income, economic activity, social networks, and neighborhood characteristics (Flanagan et al. 2011; Spielman et al. 2020).

Given the same exposure to external environmental hazards, different population groups may vary in their sensitivity and resilience (capacity to respond and recover from a disaster) due to social and demographic characteristics (of people and households) associated with social vulnerability in the context of their respective societies. The spatial concentration or agglomeration of social vulnerability in communities and built environments with higher risks is the driver that magnifies the role of social vulnerability in human damages (CEPAL

2016; Cutter et al. 2003; Kaztman and Filgueira 1999; ONU-CEPAL 2001; Pulido 2000; Wood et al. 2010).

Accordingly, holistic, index-based methodologies have recently been developed to facilitate the combined quantification of potential human- and structure-related impacts following a disaster. The results allow the identification of urban areas—mainly at the district or national level—that need to be prioritized in an emergency scenario (Carreño et al. 2007; Izquierdo-Horna and Kahhat 2020; Robat Mili et al. 2018) and also avoid human and economic losses through the addressing of efforts to reduce human vulnerability and increase resilience prior to an earthquake (Shapira et al. 2016).

It should be noted that urban regeneration is a line of public intervention with strong growth at the international level, which coordinates infrastructure programmes, public spaces, housing and local economic and environmental development, seeking a comprehensive improvement of the state of conservation and planning of urban areas of neighborhood scale oriented by an objective image of their heritage and urban potential. This modality of actions initiated in cities of OECD countries (Organization for Economic Co-operation and Development) has gained strong emphasis in Latin American countries promoted by multilateral organizations such as Inter-American Development Bank (IDB) and UN-Habitat, and its evaluation shows the key importance of comprehensive information systems that guide selective action on a territorially disaggregated scale, combining physical actions in line with social, economic and environmental situations. In Chile, the National Urban Development Policy has explicitly recommended and prioritized the integration into the management of social vulnerability indicators with indicators of exposure to vulnerability due to risks associated with the use of buildings in a poor state of conservation and safety. Likewise, concerning urban heritage, it highlighted the need to establish differentiated levels of restriction (use or destination) and intervention (structural modification) for urban heritage at all territorial scales of protection (CNDU 2017, 2019, 2021).

The present work contributes to the literature in the field of disaster mitigation in cultural heritage by presenting and discussing the application of a holistic approach specifically aimed at assessing the seismic vulnerability of historic urban centres by considering their physical and social dimensions in the context of the urban and local case of study. This contribution covers also the field of multi-vulnerability analysis in urban areas, through the analysis of data at the neighborhood scale, using the block as a unit of study.

Major earthquake disasters have occurred in Chile, causing irreparable losses. In addition to the damage caused by major disasters, the historic centres periodically experience scattered events of building collapses resulting in deaths and injuries of inhabitants, which are notorious from time to time in the centres of the metropolitan area of Gran Valparaíso (e.g., (Jiménez et al. 2018) and Gran Santiago (e.g., (Nuria Chiara Palazzi et al. 2022)—involving areas declared World Heritage Sites, protected areas at national level—Typical zones- and at communal level—Historic Conservation Areas).

The historic city centre of La Serena, located in the north of Chile, is selected as a case study. It corresponds to the largest historic centre protected by the Chilean State (170 ha), and its building typology, predominantly adobe dwellings, is representative of most of the historical centres of colonial origin in the country. Although medium–low overall, its 2002–2017 intercensal growth was characterized by a strong increase in the immigrant population, an ageing population and stagnating housing growth. A recent study compared ten protected heritage zones in large Chilean cities through an indicator that combines secondary data, surveys and field surveys, showing that the historic city centre of La Serena reported a medium–low revitalization index, mainly

explained by its urban and housing deterioration, despite the commercial and tourist development it was experienced in recent years (Arriagada Luco and Jeri 2021).

Methodologically, the seismic vulnerability assessment methodology proposed by (Ferreira et al. 2017a, b, c) to assess the seismic vulnerability of the façade walls of masonry buildings is used to evaluate the physical vulnerability of the buildings. The results obtained are then crossed with a social vulnerability index at the block level using a priority matrix. Social vulnerability is obtained by processing the 2017 census data to a simple normalization process. Both indices are processed through a QGIS geographic information system. Through the results of the application of this methodology, it is possible to compare the levels of vulnerability and capacities of different areas of a historic urban centre and classify sub-zones by different priorities according to the type of interaction between buildings and social vulnerability. The results of this research are presented as part of a perspective where an important key to better preventive policies is Urban Heritage Regeneration Plans, including the reduction of the vulnerability both in social and housing aspects.

2 Seismic vulnerability assessment

Before assessing the vulnerability of an element or system at risk, it is first necessary to understand the concepts that help to construct its definition. In the Disaster Risk Reduction (DRR) community, the notion of vulnerability has evolved over the last 40 years. At present, numerous disasters around the world have demonstrated that disaster risk cannot be determined by focusing only on the magnitude of a hazardous event but also on its interaction with the conditions of societies and their contexts, which determine the magnitude of the damage or loss that the physical phenomenon will cause (Birkmann 2013; Cardona 2003).

Different authors have contributed to the conceptualization and measurement of vulnerability (Birkmann 2006; Bohle 2001; Turner et al. 2003; Wisner et al. 2004). The notion of vulnerability has evolved into a concept that provides explanations for differences in the likelihood of damage or loss incurred by a hazard event in an individual, a community, a city or an entire region (Hufschmidt 2015). It is a multi-structural concept composed of different key factors (exposure, susceptibility, lack of resilience) and multiple thematic dimensions (physical, ecological, social, cultural. institutional, etc.) (Birkmann et al. 2013). But it is also a multi-temporal concept as it considers characteristics of a community that enable it to anticipate, cope with and recover from a disaster (Wisner et al. 2004).

The evolution of the vulnerability concept requires the consideration of many factors which can make it difficult to understand and, therefore, to measure. Developing a system of vulnerability indicators can help translate the complexity and abstraction of the term into information that allows its evaluation, measurement and transmission to assess the impact of disasters and disseminate the results to decision-makers (UN 2005, 2015).

The following is a brief description of the assessment of physical and social vulnerability to disasters using index-based methodologies. For the case of physical vulnerability, the review focuses on the seismic hazard, which is the one used in the case study. Social vulnerability is analysed for disasters in general. This review aims to find the basis for the choice of the most suitable methodologies for this study.

2.1 Physical vulnerability

The seismic vulnerability of a structure is described by (Calvi et al. 2006) as the susceptibility of a building to damage by a ground motion of a given intensity. Susceptibility is associated with its physical and structural capacity (Maio et al. 2018). Seismic vulnerability assessment can be developed at different scales, from a single building to a large urban area. The scale of application will depend on the objective of the analysis and the detail of information required. The choice of the method to be used should be based on the selection of a simple tool that provides accurate results (Ferreira et al. 2019).

In recent years, various seismic vulnerability index methods have been developed and applied in historic centres around the world, mainly in Italy (Chieffo et al. 2022; Formisano et al. 2015; Giovinazzi and Lagomarsino 2004) and Portugal (Ferreira et al. 2013; Ferreira et al. 2017b; Neves et al. 2012; Vicente et al. 2011). These are generally based on the index method GNDT II (Benedetti and Petrini 1984) and are qualified as hybrid methods (Ferreira et al. 2019). The literature review shows that the selection of parameters is mainly related to the geometrical and mechanical characteristics of the building, the state of conservation of the structure, the presence of non-structural elements and the characteristics of the foundation soils and the immediate surroundings (Baquedano Juliá and Ferreira 2021).

Considering that out-of-plane failure is one of the most frequently triggered mechanisms in masonry buildings, (Ferreira et al. 2014) proposed a methodology to be adopted in the vulnerability assessment of masonry façade walls. This methodology proves to be particularly suitable when seismic vulnerability assessment is required in a large urban area, where there may be limitations of time, human resources, and accessibility to buildings. Subsequently, it was calibrated and three new parameters were added to the original ten in Ferreira et al. (2017a, b, c). Among its applications, its effectiveness has been demonstrated for emergency planning (inaccessible urban areas, isolated people, and possible evacuation routes), according to the generation of damage scenarios obtained from relevant seismic intensities of the study area (Anglade et al. 2020). Its contribution to the reduction of post-event urban losses as a tool for evaluating the potential benefit resulting from the application of different seismic retrofitting strategies was also demonstrated (Aguado et al. 2018). In addition, it was also recently adapted and applied by (Ramírez Eudave et al. 2022) to the unreinforced masonry building typology of Atlixco, México, where its applicability is tested through the information available in the INAH building inventory. Due to the applicability of the results and their cost-effectiveness, this tool has been selected for the analysis of the seismic vulnerability of the historic centre of La Serena.

2.2 Social vulnerability

An important discussion on the measurement of vulnerability is the integral analysis for both the environmental and social dimensions according to the scales and situations involved in the design of better public policies (global, regional, and local).

Firstly, it is important to highlight that the approach to social vulnerability has had an important development from two different sources: environmental and social perspectives and that their integration is still a work in progress. Both perspectives have sought to measure its multidimensional and multicausal meaning, considering the convergence or interaction of external pressures and internal factors, but recognize different degrees of success depending on the cases and methodologies.

On the one hand, the social perspective of vulnerability emerges from research on the social and economic crisis and its interaction with different social processes and conditions using data at the individual, household, and community levels. Research on the rapid impoverishment that occurred in Latin America during the 1980s and the informal community responses allows for the development of the AVEO scheme (Assets, Vulnerability and Opportunity Structure framework).

During the 1990s and 2000s, the study of different economic crises and their social causes and effects has continued using this perspective in the search for indices of social vulnerability that better reflect the explanatory causes and expressions of poverty and inequality. Several authors recognize that the analogy between environmental and social disruptions and community responses is an important key to the development of these theories (CEPAL 2022; Kaztman and Filgueira 1999, and many others).

On the other hand, the environmental perspective focuses on the links between environmental risks and disasters with the social vulnerability of the affected population. Such studies have expanded in the context of growing environmental awareness of climate change and emerging natural disasters. During the 1990s and 2000s, the spread of GIS, online census data and satellite resources enabled several studies on natural disasters and their effects, both in the OECD (Organization for Economic Cooperation and Development) and in developing countries.

Measures of social vulnerability (SOVI index) play an important role in the place-based framework on the development of social vulnerability, helping emergency managers to identify population groups that are most susceptible to disaster risks and discuss more effective reduction strategies to avoid human and economic losses through directing efforts and policies to reduce human vulnerability and increase resilience prior to an earthquake (Cutter et al. 2003; Mengal et al. 2021; Shapira et al. 2016).

The Social Vulnerability Index (SoVI) has been widely used to measure socially vulnerable people. The use of the aggregate index combines a set of social vulnerability indicators that can quantify the relative level of overall social vulnerability and contribute to policy formulation by identifying variables that mitigate or amplify local social vulnerability. Multi-criteria risk studies on vulnerability often integrate economic, social, and ecological dimensions by combining data production with a cartographic approach (Carreño et al. 2007; Izquierdo-Horna and Kahhat 2020; Park and Xu 2022; Robat Mili et al. 2018; Scheuer et al. 2011).

Tate (2012) identifies three commonly used configurations of social vulnerability indices: deductive, hierarchical, and indicative structures. Deductive methods commonly contain fewer than ten indicators that are normalized and aggregated into an index. Hierarchical designs have employed approximately 10–20 indicators, separated into sub-indices that share the same underlying dimension of vulnerability. Finally, the inductive configuration starts with a large number of indicators (20 or more) that are reduced to a smaller set of factors using a principal component analysis PCA.

The literature about the SOVI index recognizes two different types of studies in terms of temporality: longitudinal (over time with different zones) and transversal (once ex-post in case of natural catastrophe). In the longitudinal perspective, the objective is to represent trends in vulnerability in different zones and over time (Tate 2012). An example of this line is the study presented by Bronfman et al. (2021) who explore the spatial and temporal variations of social vulnerability in Chile over the last two decades using census data in the SoVI Index for 2464 districts across the country for 1992, 2002 and 2017. In developed countries, another example is the study on the differential

contributions of the constituent components of the Vulnerability Index over time in the Greater Houston metropolitan area in the USA (Park and Xu 2022).

This longitudinal perspective has allowed the identification of some persistent disadvantages (mobility or disability, ageing, and family structures, and recently migratory conditions). Still, it recognizes that there is an important limitation in the changing composition of small area populations related to the spatial and temporal interaction of different factors behind social, urban and economic changes in different contexts. A major challenge remains the ability to understand the dynamic nature of social and environmental risks over time. A Social Vulnerability Index used to measure the social vulnerability of a place using the same data, in the same place, may provide different results because of changes over time. (Goodman et al. 2021) modelled 28 sociodemographic variables from the American Community Survey in 4162 census tracts in Florida and concluded that the results obtained did not support the theory-driven vulnerability pillars because many of those variables showed little or no variability, limiting their explanatory power. In conclusion, there is a limitation detected for longitudinal studies coming from the great spatial heterogeneity that varies or affects the results and their expansion over time, being therefore essential to pay more attention to the changing contexts of social vulnerability (Bronfman et al. 2021; Goodman et al. 2021; Park and Xu 2022; Spielman et al. 2020).

Moreover, the transversal perspective of the case studies provides important evidence but also shows that a detailed SOVI index would always require a better understanding of the causal relationships between risk and social vulnerability in the specific contexts of both dimensions, which makes it challenging to generalize social measures across contexts (Goodman et al. 2021; Scheuer et al. 2011).

One of the best examples of transversal studies is Flanagan et al. (2011), which used a social vulnerability index (SVI) with 15 variables at the census tract level to explore the impact of Hurricane Katrina on local populations. The database was the 2000 U.S. Population and Housing Census, which, it is worth noting, offers many more variables than the Chilean census. The SVI was studied in terms of correlation with death records obtained from the Louisiana Office of Public Health and included data collected by the Hurricane Katrina Disaster Mortuary Operational Response Team. The Katrina case study illustrates that the elderly were particularly vulnerable during this event (Flanagan et al. 2011).

Another example is presented by Mengal et al. (2021), who apply a social vulnerability index for Gwadar district, Pakistan, for imminent earthquake and tsunami hazards at the level of 16 villages. A social vulnerability index map compared to the seismic-tsunami hazard maps allows the identification of communities living in at-risk areas. The overall results confirm the social and economic disparities between villages and reflect differential vulnerability to natural hazards at local and regional scales. An important case of settlements with historic values affected by seismic destruction is the 2003 Bam (Iran) earthquake, which caused the death of more than 43,000 people and left more than 60,000 homeless, where women and children were especially affected. This case reveals that before the earthquake, there was a rapid growth of the poor population associated with the construction of slums and precarious housing in the heritage zone. This highlights the lack of preventive studies to define emergency programs (GeoBytesGCSE 2007).

Beyond the contributions and limitations of the studies discussed above, we must conclude that social vulnerability recognizes types of communities, households or individuals that experience disproportionately negative outcomes following natural disasters. However, many doubts have arisen about the generalizability of social vulnerability measures, largely due to variations in socioeconomic and demographic characteristics over time and across regions (Goodman et al. 2021; Mengal et al. 2021).

Clearly, it is important to highlight the design of policy responses that use integrated social and environmental vulnerability efforts. There is an important need for programs aimed not only at mitigating damage after it has occurred but also at designing preventive policies and promoting strategic spatial planning in areas at risk. Although it is true that emergency programs tend to be a focus area for studies on vulnerability and natural disasters in international literature trends, it should be noted that urban regeneration is a line of public intervention with strong growth especially focused on urban heritage areas where there is a significant risk both from a social and building vulnerability point of view.

In fact, the Historic Centre of the city of La Serena is a case where there is some experience in emergency programs after disasters and it is also an important place for urban regeneration policies that could be strategic to prevent or reduce vulnerability. Emerging regeneration policies coordinate programs for infrastructure, public spaces, housing and local economic and environmental development, seeking a comprehensive improvement of the state of conservation and planning of neighbourhood-scale urban areas guided by an objective image of their heritage and urban potential. This modality of actions initiated in cities of OECD countries has gained strong emphasis in Latin American countries, promoted by multilateral organizations such as the IDB and UN-Habitat. Its evaluation shows the key importance of comprehensive information systems that guide selective action at a disaggregated territorial scale, combining physical actions in line with social, economic and environmental situations.

In Chile, the National Urban Development Policy has explicitly recommended and prioritized the integration in the management of social vulnerability indicators with indicators of exposure to vulnerability due to risks associated with the use of buildings in a poor state of conservation and safety. Likewise, concerning urban heritage, it highlighted the need to establish differentiated levels of restriction (use or destination) and intervention (structural modification) for urban heritage at all territorial scales of protection (CNDU 2017, 2019, 2021).

3 Seismic hazard: seismicity in the study area

Chile is one of the most seismically active countries in the world, where large earthquakes have occurred in the past and will certainly occur in the future. It is located on the western edge of the South American plate, where the Nazca and Antarctic plates converge and generate subduction zones (Fig. 1). Large subduction earthquakes with seismic moment magnitudes (Mw) close to or greater than 9.0 are referred to as mega-earthquakes because of their high hazard and destructive capacity (Contreras and Winckler 2013). The speed of convergence between the Nazca and South American plates in front of Chile varies between 6.5 and 7 cm per year. However, in the contact region between the two plates, there is no relative displacement; both plates are locked together. The convergence is always continuous, generating an elastic deformation that, when it reaches its limit, activates the contact and generates large earthquakes (Barrientos 2010).

The coastal zone of Chile concentrates more than 25% of the energy released in seismic form worldwide (Cisternas 2011). Figure 1 shows the 15 largest earthquakes that occurred in Chile over the last 200 years. They correspond to earthquakes with a magnitude equal to or greater than 7.7 Mw. The size of the earthquake (magnitude) is proportional to the area of the zone that was able to move and how much it moved (CSN 2013).
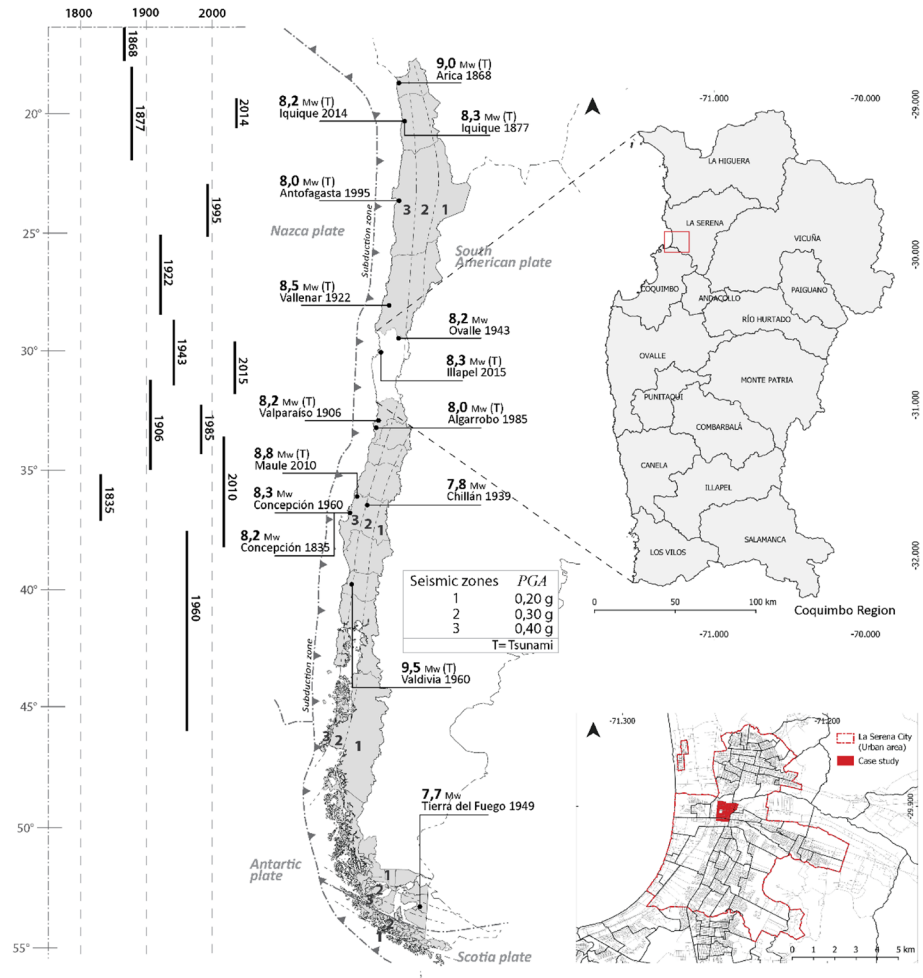
Fig. 1 Seismicity in Chile (Processed from www.csn.uchile.cl), Coquimbo region (IV Region) and case study

The Chillán earthquake of 1939 had the highest number of human losses in the history of Chile, with 5648 fatalities, and the Valdivia earthquake, in 1960, entered history as the most powerful earthquake ever recorded, with a magnitude of 9.5 Mw. Three major earthquakes have occurred in recent years, the Maule earthquake in 2010, Iquique in 2014 and Illapel in 2015, all of which have generated a Tsunami, with the one in 2010 being the most destructive. Precisely, the 2015 Illapel earthquake is the seismic event with the greatest moment magnitude that has occurred in the study area of the present paper (Coquimbo Region; more precisely, the city of La Serena).

On September 16, 2015, the Mw 8.3 Illapel earthquake occurred in the Coquimbo region (Fig. 1). The earthquake occurred on thrust faults along the boundary of the Nazca and South American plates, at a depth of 22.4 km. It was immediately followed by tsunami waves which caused severe damage to Coquimbo's seafront. The run-up depth in the bay was over 4.5 m and extended over a distance of ~500 m from the coast in some areas. The

2015 Illapel earthquake seems to have a rupture similar to the previous 1730, 1880 and 1943 events (S Ruiz and Madariaga 2018). In total, there were 13 fatalities and 6 missing persons after the event, mostly due to the tsunami although an immediate evacuation of over 1 million people likely greatly reduced the impact and casualties of the event. Despite the reported observations of erosion and scouring in the coastal border, liquefaction of loose soil deposits, settlement in bridge abutments, rock falls in steep road slopes, and more than 7000 dwellings damaged (Candia et al. 2017), this earthquake produced limited damage in modern civil infrastructure in the Coquimbo region.

Other significant earthquakes that have occurred in the Coquimbo Region are Punitaqui in 1997 (7.1 Mw) and more recently Coquimbo-La Serena in 2019 (6.7 Mw). In the 1997 Punitaqui earthquake, an MKS intensity between VII and IX was identified in the epicentre surroundings, almost 5000 adobe houses were destroyed, and about 15,700 were damaged. In the city of La Serena, the intensity was less than VI, and the affected buildings were less than 2% of the housing inventory, according to the 1992 census (Pardo et al. 2002). In the 2019 Coquimbo-La Serena earthquake, the epicentre was located 25.2 km southwest of La Serena, where an intensity value of VIII (IMM) was reported. At least 200 constructions suffered significant damage (Farías Vega 2019). This earthquake occurred in the downgoing slab of the Nazca Plate and not on the interface between the two plates, at a depth of 53 km. More details of this event can be found in Sergio Ruiz et al. (2019). Consequently, the earthquakes that have occurred in the study area have been of both intra- and interplate origin.

Regarding the damage observed during recent earthquakes, the effects of the 2015 Mw 8.3 Illapel earthquake were well-documented by different authors. Fernández et al. (2019) assessed the damage using the MSK-64 macroseismic intensity scale adapted to Chilean civil structures. 9317 dwellings were inspected, and 7285 of them showed some degree of damage. As expected, adobe and masonry constructions were the most affected by the earthquake. Candia et al. (2017) reported the main observations related to the built environment along the coasts. The tsunami waves generated during the 2015 Illapel earthquake caused moderate to severe damage to vital infrastructure in some cities of the Coquimbo region. The main observations can be summarized as follows: spread erosion and scouring in the borderline, liquefaction of loose sand deposits, settlement in bridge abutments, the response of gravity retaining structures, and several cases of rockfalls in steep road cuts. Another post-tsunami survey was conducted by Aránguiz et al. (2016).

In Chile, like in other countries, meaningful seismic resistance standards have been established following significant earthquake events. After the 1960 earthquake, the development of the first anti-seismic design standard for buildings, NCh 433, became official in 1972 (NCh 433.Of 72—Earthquake Resistant Design of Buildings, 1996). This standard establishes seismic zones according to the distance from the subduction zone between the Nazca and South American plates (Fig. 1). In zone 3, where the study area is located, it is expected that structures will be subjected to greater seismic stress in a given time frame. The highest stresses are in the coastal zones—with values up to 0.54 g—and decrease as it approaches the Andes Mountain range, down to a minimum of 0.22 g (CSN 2016).

The adoption of this standard led to the abandonment of the constructions in raw earth technique since it only considers reinforced concrete, steel, reinforced masonry, and wood buildings. This situation left unreinforced masonry constructions of adobe, stone, and rammed earth, which represent most of the country's heritage buildings, unregulated.

According to data from the Inventory of Immovable Cultural Heritage (DA-MOP 2000), more than 40% of the heritage buildings that existed in Chile until that date was built on raw earth, mainly adobe. But, in the absence of a structural strengthening and reconstruction

standard in force, many of them were lost. Following the 2010 post-earthquake emergency, the standard NCh 3332: Intervention Standard for Heritage Constructions of Raw Earth (2013) was developed. Its objective was to standardize damage assessment methods, guide the interventions of earthen heritage buildings in the reconstruction stage, and improve their structural safety conditions.

4 Background collection, inspection procedure and database

Before the fieldwork, a database was created by assigning a code (related to census entities) to the blocks and to each of the buildings within the study area. For the selection of the study area and definition of architectural typologies, different bibliographic sources were carefully analysed (Contreras Vergara 2018; Kanno and Torres 2020; Marquéz de la Plata 1979). In addition, images and reports of 2019 post-earthquake damage to the buildings in the historic centre were requested from the Council of National Monuments. This information allowed confirming details regarding, for example, the type of construction materials and the quality of the connections between the façade walls and the orthogonal structures, walls, floors and roof. The data to assess social vulnerability were obtained from the latest available census corresponding to the year 2017, carried out by INE—National Institute of Statistics, Government of Chile.

The fieldwork was carried out between November 2021 and January 2022. All buildings in the study area were externally assessed in situ to collect the necessary data for calculating vulnerability indices using a detailed checklist developed for this purpose.

The two-page survey begins with a general description of the building, including, for example, the number of floors and type of use. The following section identifies the location of the building within the block, its interaction with other buildings and the morphology of the site where it is located. Then a detailed description of the façade, dimensions, characteristics of the openings and presence of non-structural elements is provided. The materiality of the vertical and horizontal structural elements and their state of conservation is then identified. Finally, questions associated with vulnerability and fire risk assessment of each building are formulated, the results of which will be shown in future work. Figure 2 displays an example of the inspection form survey used in this work.

In the post-fieldwork stage, a multi-purpose tool connected to a relational database within a GIS environment was used to facilitate the visualization and analysis of the results. The GIS application software (QGIS 3.16) represents each block and building by its footprint to plot the results of the assessment.

5 The Historic Centre of La Serena

5.1 Selected study area

The city of La Serena has one of the most important and oldest historic centres in the country, founded in 1544. It was declared a national monument—Typical or picturesque zone category (Decree No. 499, 1981) by the Council of National Monuments (CMN)—to preserve and protect the typical characteristics of a traditional Chilean city, such as its primitive urban layout and architectural style. The historic centre, one of the largest protected areas in the country, has a surface area of 170 hectares. Its urban layout, common to other
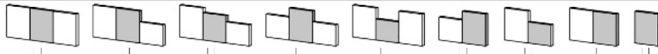
VULNERABILIDAD SISMICA Y RIESGO DE INCENDIO   Fecha:_____ Cód. edificio:_____

Dirección:_____ Descripción:_____

Tipo inspección: ☐ Exterior ☐ Parcial ☐ Completa (>2/3) **Clasificación:** ☐ Privada ☐ Pública   **Edificio estratégico:** ☐ Sí ☐ No

N° de pisos:_____	**Uso:**	1°	2+		1°	2+	**Utilización:**	N° de pers. (1er piso)_____
N° de subte:	Viv. unifamiliar	☐	☐	Escuela	☐	☐	☐ Completa	N° de pers. (2do piso)_____
Altura piso a cielo:	Viv. multifamiliar	☐	☐	Hospital	☐	☐	☐ Parcial	N° de pers. (3er piso)_____
_____	Comercial	☐	☐	Biblioteca	☐	☐	☐ En construcción	N° Total del edificio_____
Valor edificio:	Mixto (R+C)	☐	☐	Serv. Público	☐	☐	☐ Abandonado	¿N° de pers. con movilidad reducida o que necesiten asistencia? (ej:
☐ Alto	Restaurante	☐	☐	Oficinas	☐	☐	☐ En ruinas	niños, ancianos, discapacitados)
☐ Intermedio	Hotel	☐	☐	Turismo-Ocio	☐	☐	☐ No autorizada	☐ Sí ☐ No ¿Cuántos?_____
☐ Discordante	Taller/Bodega	☐	☐	Farmacia	☐	☐	☐ Subarriendo piezas	

Accesibilidad: Ancho de la calle_____ (m) (en frente del edificio)   Sentido: ☐1 ☐2   Est. autos ☐ Sí ☐ No

Historial de intervenciones: Sustitución del entrepiso ☐ Sí ☐ No (madera por hormigón)   Renovación del techo: ☐ Sí ☐ No

Interacción otros edificios:
☐ Aislado ☐ Pareado ☐ Intermedio
☐ Esquina ☐ Libre por un costado

          No Izq. Der.
Diferente tipología estruct. ☐ ☐ ☐
Desalineación entrepiso ☐ ☐ ☐
Desalineación techos ☐ ☐ ☐
Desalineación fachadas ☐ ☐ ☐

Regularidad:
En planta: ☐ Sí ☐ No   b_____ m

En elevación: ☐ Sí ☐ No   t_____ m
☐ Arcos en 1er nivel   L*_____ m
☐ Reducción área en altura
☐ Presencia de torres

Morfología del sitio:
☐ Cresta ☐ Plano
☐ % pronunciada ☐ % leve
☐ Pie de monte
¿Edificio forma parte del conjunto construido en mismo contexto histórico?
☐ Sí ☐ No

Desalineaciones fachadas (≥ a 0,5 m):

Fachada

Información general:
Espesor muro (cm):
Longitud fachada (m):
Altura total fachada (m) incluido fronton:_____
Últ. alt. tímpano (m)_____
Frontón: ☐ Sí ☐ No
Alto:_____ Ancho:_____

Revestimiento: ☐ Hormigón ☐ Cal
Dinteles: cortos ☐ Sí ☐ No
Vanos: ☐ Madera ☐ Metal

Aberturas:
Vanos de gran dimensión (mayor a 2,5 veces espesor muro) 1.5 m aprox. ☐ Sí ☐ No
Vanos cerca a intersecc. (distancia menor a 3 veces espesor muro) 1.8 m aprox. ☐ Sí ☐ No
Vanos dimensiones: ☐ regulares ☐ irregulares
Regularidad (desalineado >1/2 altura del vano)
Verticalmente ☐ Sí ☐ No
Horizontalmente ☐ Sí ☐ No
Alineados en altura ☐ Sí ☐ No
N° vanos con dist. Inf. A 1.1m_____

Radio de aberturas:

Tipo	N°	H. piso vano	Altura	Ancho
Puerta 1				
Puerta 2				
Vent. 1				
Vent. 2				
Vent. 3				

Presencia de:
☐ Contrafuertes: ☐ F. Principal ☐ laterales
☐ Ochavo ☐ Chimeneas ☐ Eq. Mecánicos
☐ Balcones ☐ Cornisas ☐ Balaustres
☐ Voladizos ☐ Letreros,etc

Sistemas estructurales

A - Adobe	B - Albañilería	P - Piedra	M - Madera	S - Acero	H – H. Armado
A1 - Adobe Simple	B1 - Simple	P1 - Simple	M1 - Marcos sin relleno	S1 – Acero arriostr.	H1 – Marcos
A2 - Adobe con refuerzo tradicional (llaves, adobe, escalerillas)	B2 - Armada o reforzada	P2 - Reforzada	M2 – Marcos / Adobe pandereta	S2 - Marcos rígidos	H2 – Muros
A3 - Adobe con refuerzo moderno (geomalla, electrosoldada, Tensores)	B3 - Confinada		M3 - Marco / Adobillo		H3 – Mixtos
			M4 - Quincha		H4- Bloques
Fachada 1er N.	Fachada 2do N.	Ochavo	Frontón	Tímpano	Muros laterales	Muros int./ Tabiques	Corredor exterior

Elementos horizontales

Entrepisos	Madera	Perf. metálicos	Losa aligerada	Losa maciza	Ancho (cm)
1°	☐	☐	☐	☐	
2°	☐	☐	☐	☐	
3°	☐	☐	☐	☐	

Tramo: Máx:_____ (cm) Mín:_____ (cm)

Techumbre:
Tipo: ☐ Plana ☐ 2 aguas ☐ 4 aguas ☐ % simétrica ☐ % Asimétrico
Materialidad: ☐ Madera ☐ Metal ☐ Bóveda mampostería ☐ H.A.
Cubierta: ☐ Tejas arcilla ☐ Zinc ond. ☐ Vegetal ☐ Tierra
Refuerzo en perímetro muro-cubierta:
☐ Tensores acero ☐ Con cadena de H.A ☐ Viga de repartición
☐ Con viga collar de madera ☐ Sin cadena, ni viga collar ni tensor

Fig. 2 Seismic vulnerability and fire risk information survey form

South American colonial cities, was planned by applying the Roman grid (in particular, the 6 by 6 Spanish urban blocks) promoted by the Laws of the Indies issued by the Spanish Crown (MVM 1973).

The selected study area has a surface area of 87 hectares, which for simplicity of analysis and data collection, was subdivided into four zones (Fig. 3b). It corresponds to the first limits of territorial occupation and has the oldest and most representative buildings of the various architectural typologies of the historic centre. Originally, about 80% of the

a)　　　　　　　　　　　　　b)
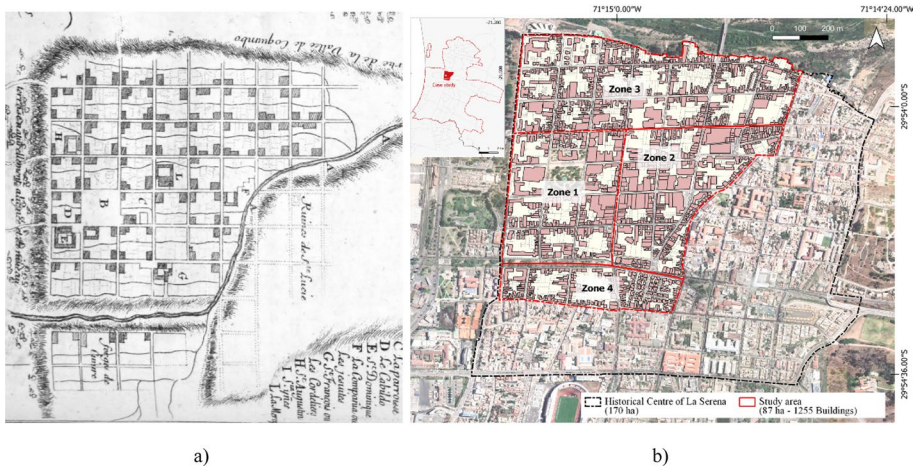
Fig. 3 **a** Map of La Serena 1713, Frezier Frezier (Marquéz de la Plata 1979); **b** Historic centre of La Serena and study area

buildings were for residential use. It is currently considered a heritage neighbourhood with mixed land use, with a high presence of commercial areas, and only 40% of the buildings have residential use (CMN 2010).

Zone 1 corresponds to the foundational blocks. The main government institutions, museums and banks are located here. There are large houses that originally occupied 1/8 of the block; nowadays, they are used for schools and commercial and services buildings mainly. Zone 2 has a strong commercial character since the colonial market, currently known as *La Recova*, is located in this zone. In both areas, there is a great diversity of economic and productive activities, which is reflected in a high pedestrian and vehicular flow and a high floating population during the day. Zones 3 and 4 correspond to areas that keep their original residential function; nowadays, approximately 70% (1274 out of 1857) of the total population of the study area is concentrated here (INE 2017).

5.2 Building characterization

The study area is composed of 1255 buildings, 636 (51%) of them correspond to traditional masonry buildings and 619 (49%) to reinforced concrete or other modern structures, which were not considered in this analysis since "modern" buildings are out of this study's scope. However, it is worth mentioning that a large percentage of these buildings have a high heritage value as they represent the urban renewal period between 1948 and 1952, known as "*Plan Serena*" (Fig. 4).

In the group of traditional buildings in the study area, two highly representative architectural typologies can be recognized, which are related to a specific building period and social context. These are i) Colonial derivation typology (until 1840) and ii) Classical derivation typology, which is divided into two styles, Classical (1830–1860) and Classical *Serenense* (1850–1880) (Fig. 5).

In terms of materiality and volumetry, the two typologies keep the characteristics of the traditional Chilean house, present in various historic centres of the country, mainly from the Atacama to Ñuble Region. They are mainly 1-storey, with regular L or
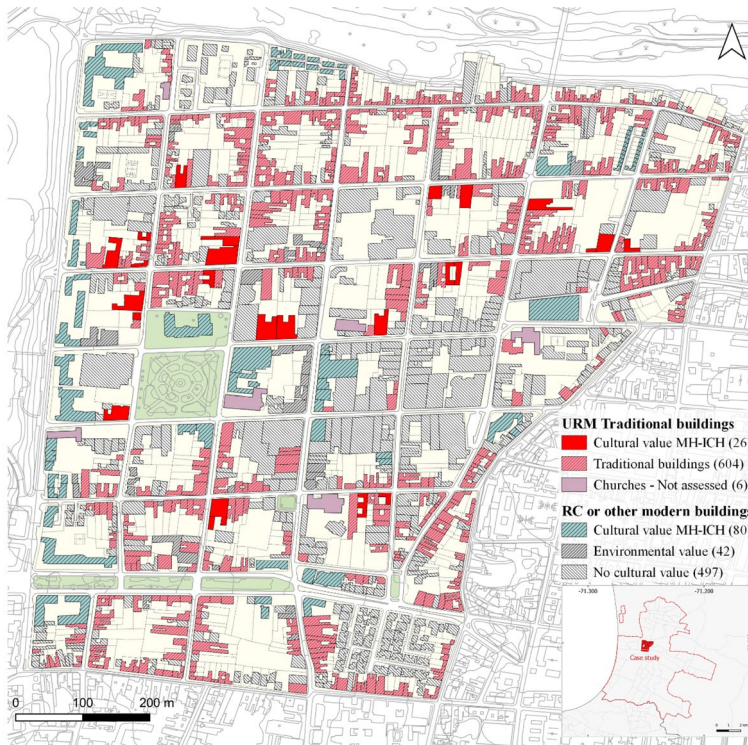
Fig. 4 Identification of the buildings assessed in this study

a)   b)   c)

Fig. 5 a Colonial Typology (Photo: Daniel Contreras); **b** Classical derivation typology: Classical (Photo: Marta Carvajal Alvarez); **c** Classical derivation typology: Classical Serenense

C-shaped floors, with the rooms aligned around 1 or 2 courtyards, the main volume has a gable roof aligned toward the street, and the dwellings are in aggregation, forming a continuous façade that originally completed the block. Like most traditional buildings in Chile, the buildings under study have load-bearing adobe masonry façade walls. The most used adobe block measures $60 \times 30 \times 10$ cm and is laid in the header bond. In order to reach greater heights and keep a slenderness ratio between 1:8 and 1:7, the walls increase up to 90 m in thickness (Fig. 6a), measurements that arise from the modulation
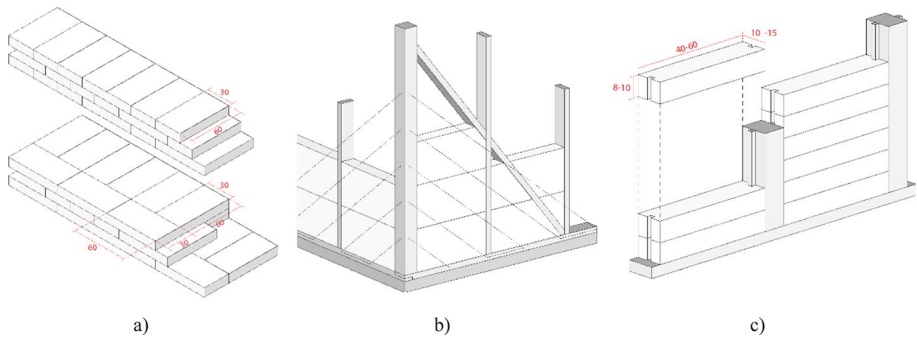
Fig. 6 a Different thicknesses of the walls with $60 \times 30 \times 10$ cm block size; Mixed timber structure **b** filled with adobe laid on rowlock stretcher bond; **c** Adobillo

of the block (Rivera 2017). The buildings increased in height using timber framing filled with adobe laid on rowlock stretcher bond (Fig. 6b) or *adobillo* (Fig. 6c).

(i) Colonial derivation typology (CO)

Although Colonial buildings are characterized by an austere design, some recurrent structural, functional and ornamental elements can be recognized, such as the stone arched doorways (located in the main access of the building, generally in a centric position on the main façade and the cornerstone pillar (which fulfils the function of allowing double access to the commercial areas and at the same time supporting the masonry above (Fig. 5a). Most of the buildings observed have large spacing between openings, which sometimes do not coincide in height. Above the openings, there is typically a wooden lintel made of four or more pieces (aligned to cover the width of the wall) with the ends embedded in the adobe masonry.

Correspond to one-storey structures with adobe load-bearing walls without embedded timber reinforcement. The colonial settlement was a homogeneous set of constructions contiguously arranged and mutually interconnected. The connection between the façade and the orthogonal walls is made through the interlocking of adobe bricks in the intersections. For this reason, original masonry structures presented good connections between the main-adjacent façades and the façade-orthogonal wall. Nevertheless, the urban growth process resulting from the real estate boost installed over the last 30 years has led to heavy changes in the internal spaces of these structures, which, in turn, have resulted in structural discontinuities on the original buildings and urban blocks. These alterations, with inadequate or null repair interventions after past earthquakes, have direct implications on the seismic performance of modified URM buildings, leading to a larger risk of local collapses due to the activation of out-of-plane failures in the case of poor connections between walls and parts of them (Fig. 7a).

The roof structure is made of king trusses and a collar tie, originally covered with wooden tiles and an eave overhanging the line of the façade, an effective solution to prevent rainwater from filtering into the adobe walls and maintain the quality of the masonry. The main seismic vulnerabilities observed in colonial-style structures are the absence of ring-beam at the top of walls which would avoid concentrated roof loads and allow their

Fig. 7 a Poor interlocking connection of the adobe bricks at intersections; **b** impulsive nature of the roofing structure

correct distribution (Fig. 7b); the lack of adequate gables-top of walls connections; and the presence of large and heavy masonry spandrel which overloads timber lintels.

(ii) Classical derivation typology (CL)

Classical style buildings are one- or two-storey, usually maintaining the spacing between openings of the colonial style, but with more regularity in size and height. In the corner, the *ochavo* is used to replace the corner pillar. In the classical *Serenese* style, greater symmetry and height are applied to the façade. It also increases the height of the openings and decreases the spacing between them.

The singe-storey buildings have adobe masonry walls with timber elements inserted at the lintel level and along the top of the façade walls (ring beam) and at each corner (corner key). This traditional seismic resistant technique—a "ladder" placed horizontally in the wall thickness—provides effective connections among orthogonal walls (Fig. 8a). Exploiting the mechanical properties of wood, timber ring beam, and corner key in adobe walls improve their out-of-plane bending capacity and in-plane shear resistance (Misseri et al. 2020; Tolles et al. 2002). The failure of woodworking joints—hooked scarf (the connection between wooden horizontal elements, joining two
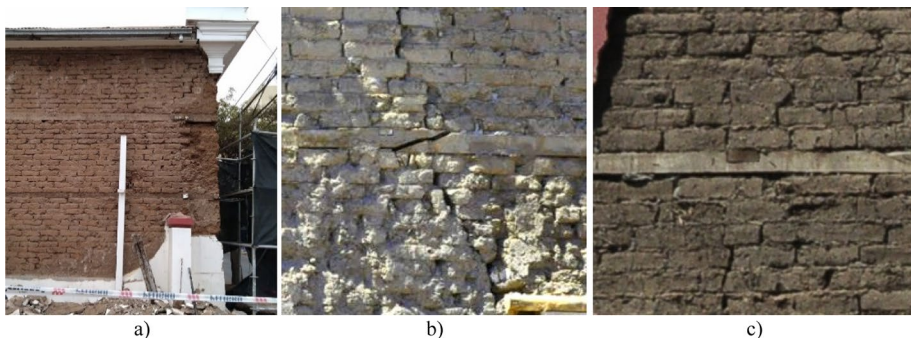
Fig. 8 CLd typology: **a** corner wall; Traditional timber joints: **b** hooked scarf and **c** halved joint (Photos: Nuria Chiara Palazzi)

members end-to-end in Fig. 8b and halved (joining two orthogonal members by removing material from each at the point of insertion so that they overlap in Fig. 8c joints—are one of the main seismic weakness of this mixed wooden-earth system when subjected to the seismic motion (Misseri et al. 2020; N.C. Palazzi et al. 2021). In fact, the link failure determines the propagation of vertical and diagonal cracks along the entire height of the wall and the activation of out-of-plane mechanisms.

The load-bearing system of the upper floors is typically made of a mixed structure of masonry and timber. The timber structure is composed of pillars (cross-section piers with 0.15×0.15 m^2) spaced between 40 and 60 cm braced with diagonals filled with earth bricks. Post-earthquake crack patterns have generally shown that mixed timber and earth structures trigged local mechanisms and partial collapse of adobe or *adobillo* due to poor links with wooden piers and masonry blocks (Fig. 9a).

The horizontal diaphragms observed are made of timber. The floor structure is composed of beams placed over a primary ring beam of the first-floor adobe walls (Fig. 9b). No metal connectors were identified between timber pieces and the adobe to improve their connection, so it is assumed that the buildings have flexible diaphragms with a weak connection to the wall.

In this study, the roof structure is considered to have an impulsive nature, as most of them have a slope of more than 30%, and despite the existence of beams at the top of the adobe wall, it is not always possible to ensure the existence of the collar beam, as the continuity of these is usually interrupted by the lateral adobe gables (Fig. 10a).

In the classical *Serenese* period, the use of carpentry gables, balustrades and cornices as façade terminations was widespread. In many buildings, the rainwater system was concealed behind wall cladding (lime or concrete) and large wooden cornices. Due to the difficulty in maintaining the rainwater gutters, there is a high probability of water penetrating the wall, causing erosion of the adobe blocks and decay of timber elements (Fig. 10b), which facilitates cracking and decreases the strength of the structural system. This problem also occurs in buildings that present architectural style renovations with the popularization of the Art Deco style after 1930. This incorporated heavy parapets (made by timber frame infill of adobe laid in rowlock stretcher bond), which have a high propensity for out-of-plane collapse due to their lack of connection with the façade and the impulsive nature of

a)   b)
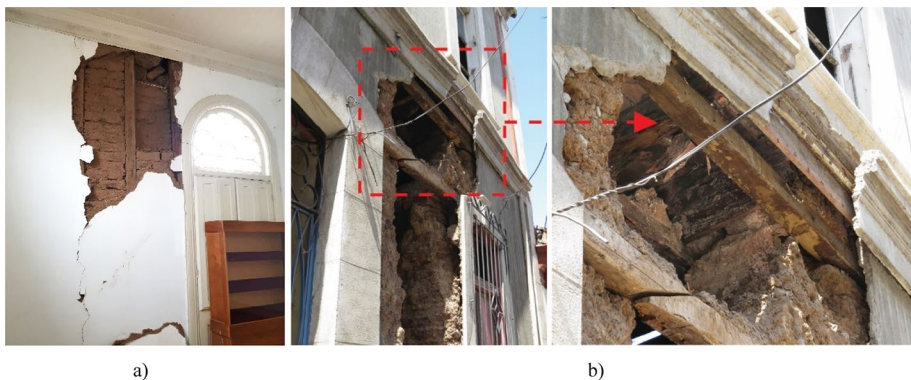
Fig. 9 **a** Timber frame infill with Adobillo; **b** Timber floor structure. Images captured after the 2019 earthquake
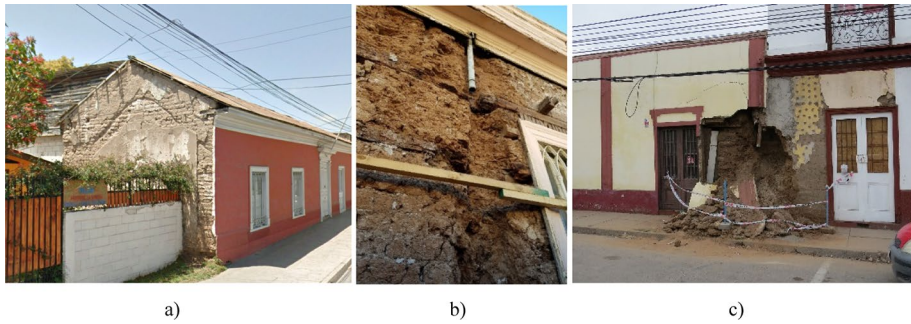
Fig. 10 **a** Impulsive nature of the roof; **b** Eroded adobe façade of CL Serenense style; **c** Adobe erosion in a refurbished building (Photo: Daniel Contreras)

the roof. Figure 10c displays the partial collapse of two façades that occurred after a heavy rainfall event in July 2022.

6 Seismic vulnerability and damage scenarios

As previously mentioned, the assessment of the physical vulnerability was performed by adopting the vulnerability Index method proposed by (Ferreira et al. 2017b). The application of this method involves the evaluation of 13 parameters (Table 1), which assess the vulnerability response of façades based on the individual evaluation of their geometric, mechanical and conservation characteristics. The parameter weightings used in this methodology are based on both experimental results and observed damage scenarios.

Each parameter is given a class, C_{Vi}, of increasing vulnerability, A (0), B (20), C (20) and D (50). The I_{Vf}^* can be then obtained by the weighted sum of the 13 parameters, each one of them affected by a weighting factor, p_i, which depends on the relative importance

Table 1 Vulnerability Index with the associated parameters' classes and weights

Parameters	Class, C_{vi}				Weight, p_i	Relative weight
	A	B	C	D		
P1 Façade wall geometry	0	5	20	50	0.50	16.7/100
P2 Wall slenderness	0	5	20	50	0.50	
P3 Area of wall openings	0	5	20	50	0.50	
P4 Misalignment of wall opening	0	5	20	50	0.50	
P5 Interaction between adjacent façade walls	0	5	20	50	0.25	
P6 Masonry quality	0	5	20	50	2.00	31.5/100
P7 State of Conservation	0	5	20	50	2.00	
P8 Replacement of the original floors	0	5	20	50	0.25	
P9 Connection to orthogonal walls	0	5	20	50	2.00	33.3/100
P10 Connection to horizontal diaphragms	0	5	20	50	0.50	
P11 Impulsive nature of roofing system	0	5	20	50	2.00	
P12 Non-structural elements	0	5	20	50	0.50	18.5/100
P13 Improving elements	0	5	20	50	−2.00	

of that parameter, Eq. (1). For ease of use, the vulnerability index is usually normalized to range between 0 and 100; the lower its value, the lower the seismic vulnerability of the façade wall (Ferreira et al. 2017b).

$$I_{Vf}^* = \sum_{i=1}^{13} C_{Vi} \times p_i \tag{1}$$

Although this methodology has already been widely applied in several geographies, the application to adobe masonry buildings in Latin American countries is still scarce. To reduce the uncertainty in the vulnerability results obtained for Chilean buildings, it became necessary to slightly adapt the vulnerability classes, integrating the recommendations of the Chilean standard (NCh 3332, 2013)—Structural Design—Retrofitting of Historic Earth Buildings—Requirements for the Structural Design Planning. This standard establishes the minimum requirements to be fulfilled by a structural project for the intervention, renovation, recovery, strengthening, restoration, rehabilitation, or structural consolidation of earthen constructions with heritage value. Recommendations from Peru's National Building regulations, technical norms (NTE.080, 2017) and other studies are also considered. The modified parameters are presented in Appendix 1.

6.1 Application of the vulnerability index methodology

The adapted façade vulnerability assessment method was applied to 718 façades on 630 buildings in the historic city centre of La Serena. The compilation of the data and analysis of the parameters yields the distribution of classes (A to D) in each parameter (Fig. 11). Although the parameters were assessed by experts and through direct observation, this type of analysis is not free of inaccuracies and uncertainties. Assigning classes of some of the vulnerability parameters can sometimes be a complex task because the structural elements to be assessed are not always available for visual inspection. Figure 11 shows that some parameters have a lower and an upper vulnerability bound. This variation is mainly due to the level of uncertainty in the construction characteristics of the buildings that cannot be clearly assigned to one of the three predominant architectural typologies of the study area (Colonial, Classical or Classical *Serenese*).

Table 2 includes the uncertainty scale used in this analysis. This scale represents the quality of the information to answer each parameter. Parameters with a high level of
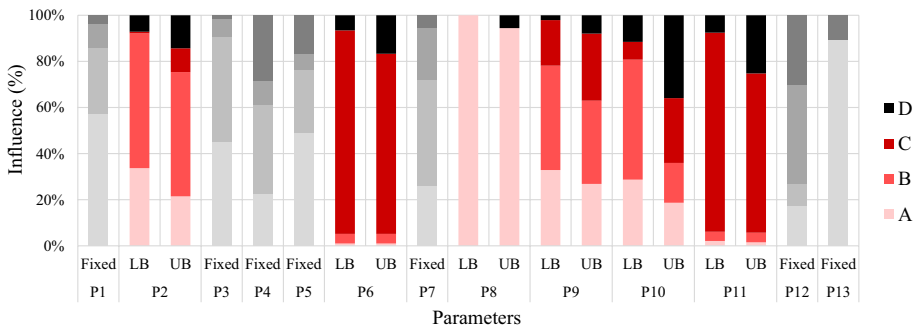
Fig. 11 Vulnerability index distribution of the building stock: Histogram and normal distribution

Table 2 Definition of uncertainty levels

Quality of the information	Parameters	Description	Possible variation (Lower and upper bound)
High (H)	P1–P3–P4–P5–P7–P12–P13	Information observed directly in situ	None (remain stable)
Moderate (M)	P2–P6–P9–P10–P11	Information inferred from photographs, buildings' planimetry and reliable oral sources and on informed assumptions based on the building typology	Lower bound is defined according to architectural typology characteristics. Upper bound is defined by the uncertainty on the characteristics of the buildings belonging to undefined building typologies (one class decrease in relation to the average)
Low (L)	P8	Absence of information	No information is available (lowest and highest limits correspond to classes A and D, respectively)

information correspond to data easily acquired in situ that do not allow assumptions to be made (stable classes). Parameters that are collected through information deduced from photographs or according to architectural typology are of moderate information quality. Finally, for parameters with no information available, the lower and upper limits are considered as class A and D, respectively.

Figure 11 shows that, for Parameter P4, Misalignment of openings, about 29% (205) of the façades are inside class D. The majority of those (179) are due to the presence of openings greater than 1.5 m wide, of which approximately half are extensions in width, due to conversion from residential to commercial use. In P6, Masonry quality, 88% (634) of the façades are assigned a class C at the lower boundary, corresponding to adobe masonry laid on header bond and good quality mortar and 7% (47) class D. At the upper bound, buildings with art deco style updates with signs of deterioration are considered as class D, increasing the number of class D buildings to 17% (120). The nature of the roof, P11, is one of the parameters classified according to architectural typology. At a lower limit, 86% (620) of the buildings are class C, corresponding to rehabilitated Colonial or Classical derivation buildings, with a roof of impulsive nature and the presence of a perimeter beam at the top of the wall. As a conservative measure, buildings without a clear architectural typology are assigned to class D. As for P12, which measures the presence of non-structural elements, 30% (218) have heavy elements on the façade, mainly parapets and balustrades, and are classified as Class D. Finally, in P13, Improvement elements, only 11% of the façades present structural strengthening actions, these correspond to integral structural consolidation projects approved by the CMN, following the recommendations of NCh 3332 (2013).

6.2 Seismic vulnerability results

The histogram resulting from the analysis for the lower (LB) and upper (UB) bounds are given in Fig. 12. A mean LB seismic vulnerability index, $I_{vf,mean}$, of 36.28 was obtained. The minimum value of the vulnerability index is 9.07, and the maximum value is 85.19. The associated standard deviation value, σ_{Ivf}, is 11.11. About 15% (107) of the façades have a vulnerability index over 45. With respect to the upper bound, the mean UB seismic vulnerability index is $I_{vf,mean}$, is of 41,64, the minimum value is 9.07, and the maximum is 88.52. The standard deviation value σ_{Ivf}, obtained for this distribution is 13.55, with about 40% (284) of the façades having a vulnerability index value greater than 45.

After the vulnerability index of each façade, I_{Vf}^*, is obtained, it is possible to estimate the expected mean damage grade, μ_D according to different macroseismic intensities.
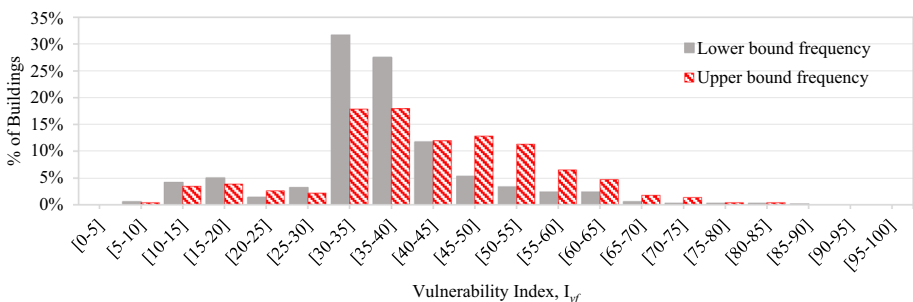

Fig. 12 Histograms with the distribution of the vulnerability index values

Equation (2) correlates the seismic hazard with the mean damage grade ($0 < \mu_D < 5$) of the damage distribution in terms of vulnerability value (Ferreira et al. 2014):

$$\mu_D = 2.51 + 2.5 \times \tanh \left(\frac{I + 5.25 \times V - 11.6}{Q} \right) \tag{2}$$

$$V = 0.592 + 0.0057 \times I_{Vf}^* \tag{3}$$

$$f(V,I) = \begin{cases} e^{V/2 \times (I-7)}, I \leq 7 \\ 1, I > 7 \end{cases} \tag{4}$$

where I is the seismic hazard, originally based on the European macroseismic intensity scale (EMS-98). In this study, the Modified Mercalli Intensity (*MMI*) scale is used, which has a direct equivalence with the EMS-98, according to (Musson et al. 2010). Equation (3). relates the vulnerability index (I_{Vf}^*) obtained through Eq. (1), to the Vulnerability index (V) used in the macroseismic method and in determining the mean damage grades (μ_D). A correction factor is determined by the function $f(V,I)$, which is introduced when the seismic intensity I is lower or equal to 7, see Eq. (4).

The ductility factor Q is associated with the ductility of a certain constructive typology—ranging from 1 to 4. In previous application of this methodology in Portugal and Italy, this value was assumed to be 2.5 or 3.0 for unreinforced stone masonry buildings (Bernardini et al. 2007; Ferreira et al. 2017b; Vicente et al. 2011). The Chilean standard NCh 433, however, establishes that the ductility of the building is related to a variable R, a response reduction factor that for masonry buildings is given by Eq. (5), whose value should be taken as 2.0 for any non-specified structure or material, as is the case of adobe. Accordingly, a ductility of $Q = 2.5$ was considered in this research.

$$R = \sqrt{2Q - 1} \tag{5}$$

To simplify the interpretation, the mean damage grade (μ_D) can be related directly to a discrete damage grade (D_k), as per (Grünthal 1998). This relationship can be associated with a Damage Factor (DF), which represents the cost necessary to return the building to its original undamaged state. The correlation can be approximated by Eq. (6), proposed by Bramerini et al. (1995) (Fig. 13).

$$\mu_D = 5 \times \mathrm{DF}^{0.45} \tag{6}$$

The correlation between discrete damage grades (D_k), damage factor (DF), mean damage grade (μ_D), and the definition of damage modified to façade walls by Ferreira et al. (2014) is given in Table 3.

Once the seismic vulnerability of each façade has been characterized, the damage distribution is estimated for different macroseismic scales. Using Eq. (2), vulnerability curves are plotted considering three values of the vulnerability index distribution (Fig. 14): the mean value and the upper and lower range limits ($I_{vf,\mathrm{mean}} - 2\sigma_{Ivf}; I_{vf,\mathrm{mean}}; I_{vf,\mathrm{mean}} + 2\sigma_{Ivf}$).

Figure 14 shows the damage distribution obtained for the representative macroseismic intensities from $I_{\mathrm{MMI}} = \mathrm{VI\ to\ IX}$, for the average values of the upper and lower vulnerability bound. In general, the average damage of the façades, at the lower bound, increases by one degree of damage with increasing macroseismic intensity. For the
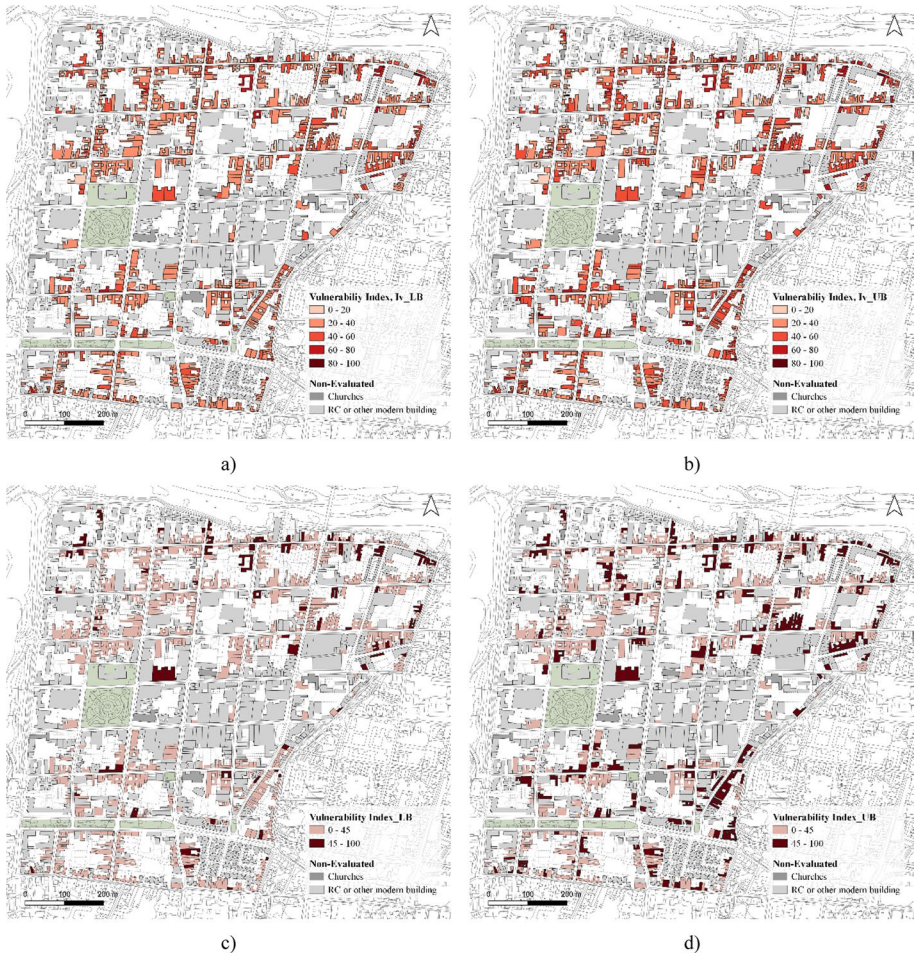
Fig. 13 Global vulnerability distribution: **a** LB; **b** UB. Façade walls with I_{vf} values over 45: **c** LB; **d** UB

earthquake scenario of $I_{MMI} = VI$, about 83% of the façades present nor or slight damage (D_1); for $I_{MMI} = VII$, about 90% of the façades present moderate damage (D_2); for $I_{MMI} = VIII$, 85,5% present severe damage (D_3); and for $I_{MMI} = IX$, the majority of the façades, about 68,4%, present very severe damage (D_4). The upper limit of vulnerability also shows a uniform variation for $I_{MMI} = VI$, VII and VIII The majority of the façades (between 60 and 70%) increase by one level of damage as the macroseismic intensity increases. The only exception is for the scenario of $I_{MMI} = IX$ where, for the upper limit of vulnerability, about 43% of the façades could present very severe damage (D_4) and 50% could collapse (D_5). Figure 15 shows the spatial distribution of the mean damage grade values for $I_{MMI} = VI$ and IX, obtained for the upper bound of vulnerability, i.e., considering the most conservative scenario.

Table 3 Correlation between discrete damage grades, D_k, and ranges of mean damage grade, μ_D (Grünthal 1998)

Discrete damage grades, D_k	Damage factors, DF	Mean damage grades, μ_D	Description
D_0—No Damage	0.00	0.00–0.50	No Damage
D_1—Slight damage	0.01	0.50–1.42	Presence of very localized/hairline cracking
D_2—Moderate damage	0.10	1.42–2.50	Cracking around door and window openings; localized detachment of wall covering (plaster, tiles, etc.)
D_3—Severe damage	0.35	2.50–3.50	Openings of large diagonal cracks; significant cracking of parapets; masonry walls may exhibit visible separation from diaphragms; generalized plaster detachment
D_4—Very severe damage	0.75	3.50–4.00	Extensive cracking in façade walls with large areas of openings, partial collapse of the façade (shear cracking, disaggregation, etc.)
D_5—Destruction	1.00	4.00–5.00	Total in-plane or out-of-plane failure of the façade wall

Description of damage grades for masonry façade walls (Ferreira et al. 2014)
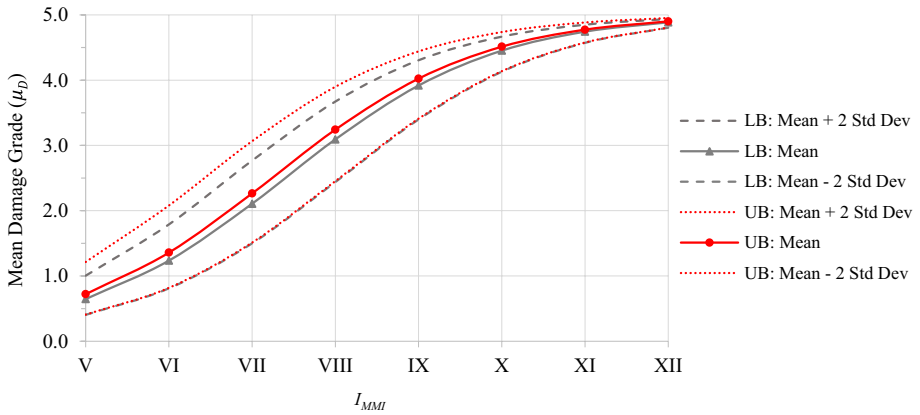
Fig. 14 Vulnerability curves for the LB and the UB seismic vulnerability index
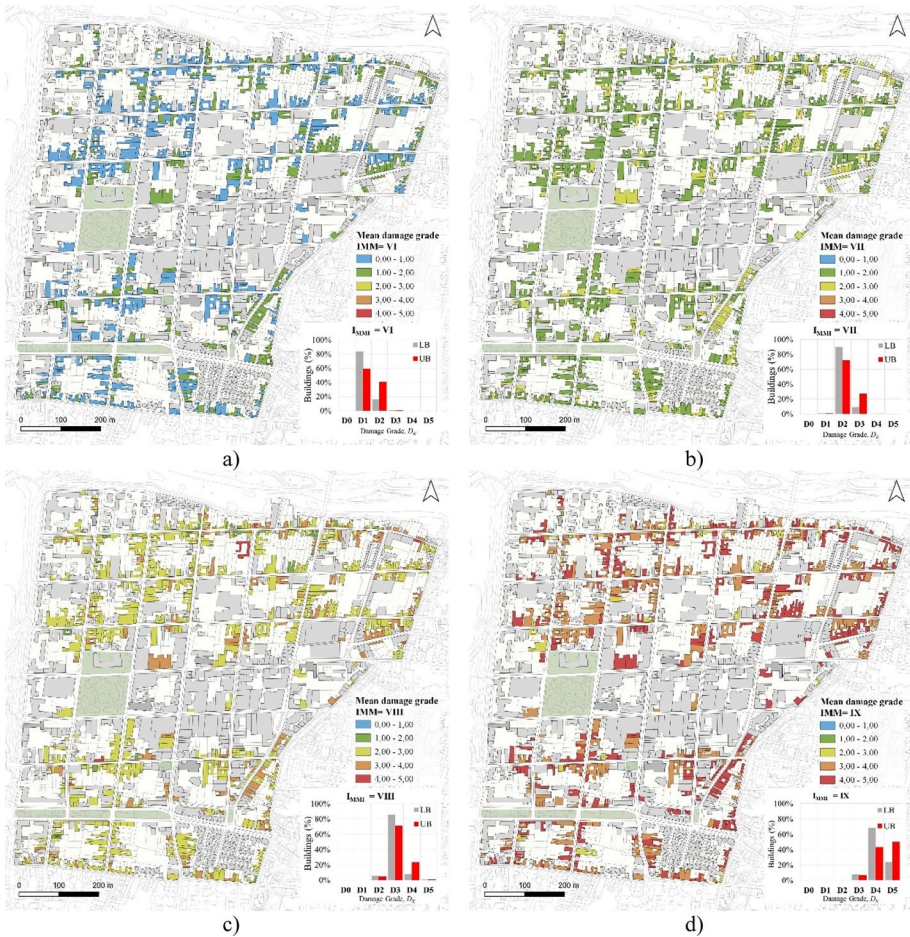
Fig. 15 Damage distributions for seismic scenarios and UB maps: a $I_{MMI}=$ VI; **b** $I_{MMI}=$ VII; **c** $I_{MMI}=$ VIII; **d** $I_{MMI}=$ IX

6.3 Fragility curves

The fragility of buildings is related to their seismic vulnerability, which can be quantified by means of fragility curves. Fragility curves are the graphical representation of the *beta* cumulative distribution function of the probability of reaching or exceeding different states of damage under a given seismic intensity (Federal Emergency Management Agency (FEMA), 1999). The discrete probability, $P(D_k) = d$, can be derived from the difference of cumulative probabilities, $P_D[D_i \geq d]$, applying Eq. (7).

$$P(D_k = d) = P_D[D_k \geq d] - P_D[D_{k+1} \geq d] \tag{7}$$

Figure 16a shows the fragility curves obtained for the lower ($I_{vf,\text{mean}LB} = 35{,}61$) and upper ($I_{vf,\text{mean}UB} = 41.64$) limit mean vulnerability distribution. In a seismic scenario of intensity VIII, there is a probability that between 80 and 85% of the façades will show severe damage (D_3), such as the appearance of large diagonal cracks, significant cracking in parapets or generalized detachment of plaster.

The probability of some façades collapsing can be directly represented by the damage D_5, as indicated in Eq. (8). where $P(D_5)$ is the probability of the façade wall reaching the damage grade D_5.

$$P\text{collapse} = P(D_s) \tag{8}$$

Figure 16b depicts the collapse probability curves for three vulnerability distribution values ($I_{vf,\text{mean}} - 2\sigma_{Ivf}; I_{vf,\text{mean}}; I_{vf,\text{mean}} + 2\sigma_{Ivf}$) for the LB and the UB seismic vulnerability index. It shows that at macroseismic intensity $I_{\text{IMM}} = $ VIII, the maximum probability of collapse is around 15% of the façades. If the mean vulnerability values are considered, the probability of total collapse is very low, showing less than 2% for both limits (LB and UP). For proper emergency disaster management, it is important to consider the high probability of façades that could present severe (D_3) and very severe (D_4) structural damage (see Fig. 16a), which represent the risk of a partial collapse of elements with the possibility of harming people at the assessment stage. At intensity $I_{\text{IMM}} = $ IX, the values increase, showing a probability of collapse of 15–20% between the LB and UB. And for intensity $I_{\text{IMM}} = $ X, the probability increases considerably, showing a probability of collapse of between 55 and 61% of the façades.
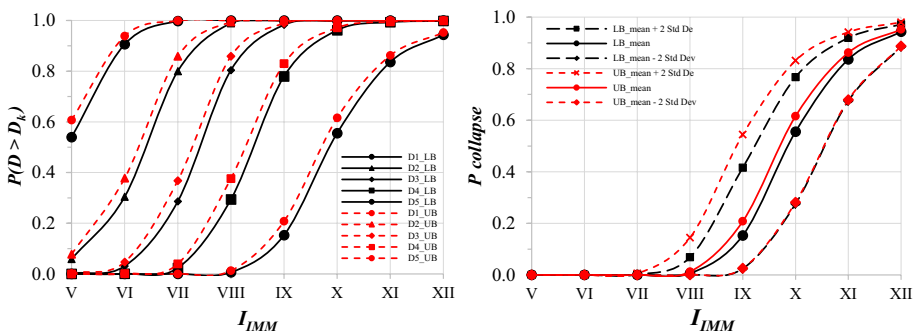
Fig. 16 a Fragility curves obtained for $I_{vf,\text{mean}LB}$ and $I_{vf,\text{mean}UB}$; **b** Probabilities of collapse for different vulnerability index values

7 Characterization of the social vulnerability

The conceptual definition of social vulnerability proposed by Wisner et al. (2004) is adopted in this work. According to these authors, social vulnerability is understood as the set of characteristics of a person or group and their situation that influences their capacity to anticipate, cope with, resist and recover from the impact of a natural hazard (an extreme natural event or process). In other words, social vulnerability is determined by the characteristics or attributes that increase the likelihood of a population suffering regressive effects in the face of a hazard and their capacity to recover from it.

The selection of variables associated with social vulnerability should be based on key social indicators of the specific regional and social context. In the US, the literature provides examples of studies using several domains that form the basis of the SVI, including census data on (i) Socioeconomic Status (income, poverty, employment and education); (ii) Household Composition/Disability (including age, single parenthood and disability); (iii) Minority/Language Status; (iv) Housing (housing structure, overcrowding) and (v) Transportation (access to vehicles). In the case of Chile, the 2017 Census database is accessible but does not include many of the domains listed above. In addition, it is also important to mention that we consider that the use of data on housing structures included in the census does not apply as an indicator of social vulnerability for this study because it duplicates or repeats data on building vulnerability.

Demographic characteristics are an important indicator for all phases of risk, from compliance with evacuation rules during an event to long-term recovery success after the event, as socially vulnerable people are more likely to die in a disaster and less likely to recover after it (Juntunen 2006). The index presented here selected only five variables (Table 4) for simplicity over the defined human population groups and for internal independence between them (less statistical intercorrelation, in other words). The description of the variables is mainly based on (Cutter et al. 2003).

Indicators were selected on the relative importance of women in the population, dependent population (under 15 and over 64), indigenous people and international migrants (foreign population), all of which have a positive relationship with social vulnerability, except for the active or working age population (15–64), which has a negative association. In all these variables, there is a strong association between poverty and social vulnerability according to household surveys in both Latin America (CEPAL 2022) and Chile (MIDESO/PNUD 2021).

The idea that disasters are gender-neutral phenomena (Fordham 1998) has been overturned for the past 20 years by including the effects of gender stratification and women's experiences in disaster research and social vulnerability analyses. It remains a reality that women earn less and have increasingly precarious jobs. At the same time, they are a key yet invisible presence in household management, especially in poorer regions (de Araujo Pinheiro 2020). This leaves them with fewer resources for recovery. Moreover, in the evacuation stage, in many cases, the priority is to protect the people in their care, such as children and the elderly (Villarreal and Meyer 2020).

According to a study presented by Sánchez-González and Egea-Jiménez (2011), the degree of social vulnerability in old age is expressed through fragility and defencelessness in the face of natural and anthropic risks, physical and psychosocial alterations in the habitability of the surroundings of the home and neighbourhood (modifications and deterioration of the environmental context), social transformations (loss of family and social networks of informal help) and cultural transformations (functional illiteracy associated with

Table 4 Variables used for the social vulnerability index

Variable description	Component name	Description and contribution	Scale and source
Percentage of women in the population	Female index	(+) Women can have a more difficult time during recovery than men, often due to sector-specific employment, lower wages, and family care responsibilities	Census blocks—INE Census, 2017
Percentage of dependent population (under 15 years old and over 64 years old)	Dependants	(+) Extremes of the age spectrum affect the movement out of harm's way. Parents lose time and money caring for children when daycare facilities are affected; the elderly may have mobility constraints or mobility concerns, increasing the burden of care and lack of resilience	Census blocks—INE Census, 2017
Percentage of the active population (working age 15–64)	Active population	(−) It is associated with access to resources to cope with an emergency and resilience. It tends to decrease social vulnerability	Census blocks—INE Census, 2017
Percentage of the population that identifies itself as being indigenous ethnicity	Ethnicity	(+) Possible language and cultural barriers affecting access to post-disaster resources and residential locations in high-hazard areas	Census blocks—INE Census, 2017
Percentage of the foreign population	Immigrants	(+) It is associated with a lack of access to resources, cultural differences, and social, economic, and political marginalization	Census blocks—INE Census, 2017

Table 5 Example of the social vulnerability index (SVI) calculation

Component name		% Active population (−)	% Ethnicity (+)
Minimum value		33.33	0.00
Maximum value		85.18	15.38
Range (Max–Min)		51.85	15.38
Interval (divided into 3 SVI Levels)		17.28	5.12
SVI levels	Rating	Range	Range
High	1.0	33.33–50.61	10.26–15.38
Moderate	0.6	50.61–67.90	5.13–10.26
Low	0.2	67.90–85.18	0.00–5.13

problems of use and access to the Internet); institutional helplessness in retirement through the absence of pension, health insurance and dependency cover, among other factors.

In relation to ethnicity, indigenous people and international immigrants are the groups with the highest association with extreme poverty status, and children and adolescents in terms of age as well. It is important to clarify that poverty rates by gender depend on location, age and family structure. In the case of the older population, the poverty rate is also heterogeneous. However, during the last decades, it is growing on average. Both groups have mobility restrictions compared to men and younger people, which affects their mobility options. Finally, the working-age population (discounting vulnerable groups by gender, age and ethnicity) is clearly less vulnerable before, during and after natural disasters.

To obtain the index, the same procedure described by the National Centre for Disaster Prevention of the Government of Mexico—CENAPRED—is used (IMTA 2015). First, coverage percentages were obtained according to census data (Table 5). From the percentages of each variable, the maximum and minimum values were identified to determine the range between them. Subsequently, the range is divided by the number of categories in which the vulnerability condition is demarcated (high, moderate and low in this study). Thus, the value that will define the range of each vulnerability level is obtained. Finally, once the indicators have been classified, they are assigned a score ranging from 1.00 (High Vulnerability) to 0.20 (Low Vulnerability).

7.1 Application of social vulnerability index

The social vulnerability assessment method was applied in the 51 blocks that comprise the study area. The results are shown in Fig. 17a. As can be seen in the figure, four blocks present a high social vulnerability. These blocks also have a high female index (over 50% of the population) and people with some degree of dependency (i.e., people under 15 years old and over 64 years old). There are 34 blocks with moderate social vulnerability, most of them with a female population of between 15 and 36% and a high percentage of immigrant population. Finally, eight blocks show a low level of social vulnerability. In general, those have a high working population, between 70 and 80% and low rates of dependents, between 15 and 18%.

# 8 Multi-vulnerability assessment and risk management prioritization

Since the social vulnerability data are at the block level, it was necessary to find a common unit of analysis; thus, the results of the social vulnerability index were crossed with the average value of the seismic vulnerability results obtained in each block. The seismic vulnerability is associated with the seismic damage distribution estimated for an intensity $I_{IMM} = $ VIII, considering the upper boundary. As shown in Fig. 17a, 42 out of 51 blocks present a level of damage that, on average, corresponds to D_3, whereas three blocks present a level of damage corresponding to D_4, on average. Six out of the 51 blocks present a level of damage corresponding to D_0 or D_1, as a result of the reduced presence of URM buildings in those blocks.

The results of social and physical vulnerability were processed through a prioritization matrix shown in Table 6. Five levels of prioritization are established: "Neglectable", "Low", "Moderate", "High", and "Extreme". This prioritization scale is useful to identify the most vulnerable zones in the study area and facilitate decision-makers addressing human and economic resources in disaster mitigation. The results of the matrix are shown in Fig. 17b.

The results show that two blocks present negligible priority as a result of a low physical and social vulnerability. They are located in the central part of the study area, in a zone with a high commercial vocation, meaning that most buildings are new or have been significantly changed. No adobe masonry buildings can be anymore found in this area. Eight blocks were identified with low priority. They are located in the central area (3) and scattered toward the edges of the study area. Like in the previous case, most of these blocks present a high presence of commerce and equipment. In addition, 29 blocks have a moderate priority level. Finally, ten blocks have a high priority. These high-priority blocks are located toward the edges of the study area, mainly in areas recognized for their high level of deterioration. None of the blocks in the study area presents extreme priority.

Some general considerations on the priority scale are described below:

– **Extreme priority** (High PV + High SV): these are blocks that combine buildings whose façades can potentially suffer partial or total collapse and high social vulner-

a)   b)
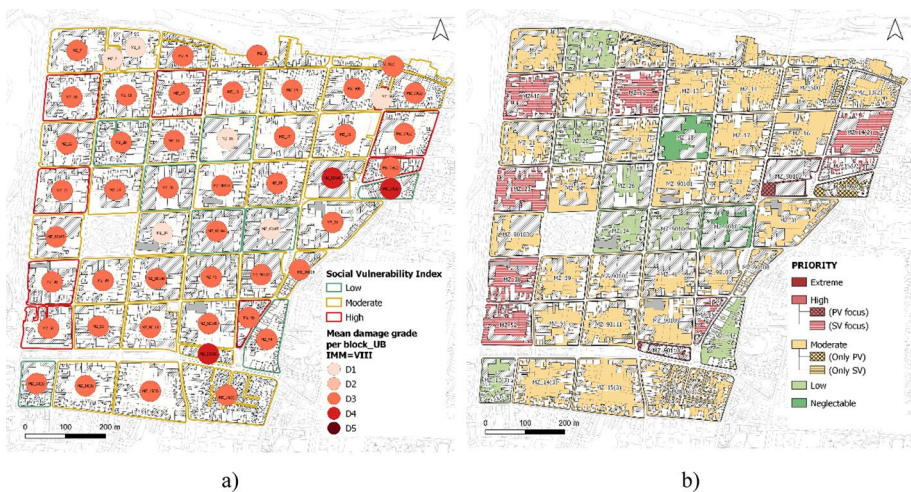
Fig. 17 **a** Social vulnerability index map crossed with the mean degree of damage per block in an earthquake scenario of intensity VIII; **b** Priority map in case of an earthquake

Table 6 Priority matrix

Seismic Physical Vulnerability (PV) Discrete seismic damage grade ($I_{IMM}=VIII$)		Social Vulnerability (SV)		
		Low	**Moderate**	**High**
Slight to moderate damage (D_{1-2})	**Low**	Neglectable	Low priority	Moderate priority (Only SV)
Severe damage (D_3)	**Moderate**	Low priority	Moderate priority	High priority (SV focus)
Very severe damage to destruction (D_{4-5})	**High**	Moderate priority (Only PV)	High priority (PV focus)	Extreme priority

ability, i.e., people that may have difficulties in responding to the emergency (reduced mobility, concern for dependents) or a weak recovery capacity due to low availability of economic resources. There is an urgent need to prioritize structural diagnostics for the implementation of structural strengthening and façade maintenance training for the community.

– **High priority: PV focus** (High PV + Moderate SV): blocks with buildings whose façades can potentially suffer partial or total collapse and the population presents a moderate level of social vulnerability. The partial or total collapse of the façade walls can lead to death or serious injury to people, as well as the obstruction of access routes for emergency vehicles. The priority level is reduced as people are more able to assess or recover from a disaster. **SV focus** (Moderate PV + High SV): blocks with buildings whose façades can potentially present severe level of damage, i.e., large diagonal cracks; significant cracking of parapets; masonry walls may present noticeable separation of diaphragms; widespread detachment of plaster, which could also cause damage to people walking on the street and collapse of rescue and evacuation routes. People can find shelter in safe areas within their dwellings. Due to the high average social vulnerability, inhabitants may present difficulties during the evacuation process and do not have the resources to recover their property, resulting in the accumulation of damage and weakening of façades in the face of possible aftershocks.

– **Moderate priority** (Moderate PV + Moderate SV): many façades can potentially present severe damage D_3, whereas the population has a moderate social vulnerability. In practice, this means that people may need help in the emergency and recovery stages but not as a priority. **PV only** (High PV + Low SV)**:** these correspond to blocks with buildings whose façades can potentially suffer partial or total collapse, but their inhabitants have a low level of social vulnerability. Investments should be made in the seismic retrofit of the buildings to reduce potential seismic damages. **VS only (**Low PV + High SV): most of the façades in the block can potentially present slight or moderate damage, i.e., in general, punctual cracks, particularly around openings, and localized detachment of wall coverings (plaster, tiles, etc.). The social vulnerability of people is high, so they may have difficulty in repairing minor damage that may increase in future earthquakes.

– **Low priority** (Moderate PV + Low SV | Low PV + Moderate SV)**:** blocks that combine buildings whose façades can potentially suffer severe damage and a population with low social vulnerability. Thus, people could have the economic resources to seismically retrofit their houses or repair them in case of a seismic event. This category also includes blocks where most of the façades can present slight or moderate damage in the case of a seismic event and are inhabited by a population with a moderate level of social vulnerability.

– **Neglectable** (Low PV + Low SV): The average damage of the façades is D_1, i.e., is expected to be neglectable or minor, and the social vulnerability of the community is low. Damage can be very localized and include light cracking with low repair costs.

9 Final remarks

Historic urban centres have characteristics that make them particularly vulnerable to natural disasters, especially seismic shaking. A large percentage of historic centres are built with unreinforced masonry or mixed structures of earth-filled timber. The seismic deficiencies

of these buildings are due to the poor quality of the materials used and poor construction practices, associated with poor connections between structural elements, out-of-plane wall collapses, in-plane shear failures and poor workmanship and maintenance (Ortega et al. 2017). However, disaster is not only a result of the interaction of the hazard with the built environment but also a result of the community's ability to cope with the emergency.

In historic urban centres, the inhabitant population often presents high levels of social vulnerability, and public interventions generally do not combine construction actions with social programmes at the block and neighbourhood scale, preferring selective rehabilitation of dwellings. This study presents the application and combination of two index-based methods for the assessment of physical and social vulnerability in a historic centre in Chile. The application of the façade seismic vulnerability index method and its adaptation to the building typologies present in the case study allowed the definition of some new parameters specific to the study area. The historic centre of La Serena is representative of the historic urban centres of Chile, so this adaptation makes it possible to replicate the assessment in many historic centres in the country, such as the Metropolitan Areas of Valparaíso and Santiago.

The application of the vulnerability assessment method for façades made it possible to obtain vulnerability curves through which it was possible to obtain the expected level of damage for different macro-seismic intensities. As a representative example, it is shown that for a macroseismic intensity $I_{MMI} = VIII$, there is a probability that between 85% (LB) and 71% (UB) of the façades will present severe damage D_3. Between 8.1% (LB) and 23% (UB) present damage D_4 (very severe) and between 0.7% (LB) and 1% (UB) of the façades could collapse completely D_5. It is important to note that special care should be taken with buildings with a mean damage grade greater than 3.5, as this could mean falling façade elements which could injure people and/or block traffic lanes for emergency vehicles.

The social vulnerability index presented selected five variables present in the 2017 census database. The application of a social vulnerability assessment method and subsequent cross-checking with the results of physical vulnerability through a priority matrix made it possible to identify the areas with the greatest vulnerability to earthquakes. This work facilitates the allocation of resources to mitigate the vulnerability of historic centres, which is often scarce and the design of regeneration programs that combines social, constructive, and urban complementary projects.

The development of such a database for different historic centres in Chile could help to reduce the uncertainty of the state of conservation and general condition of Chile's immovable cultural heritage considering the socio-demographic profiles of the population involved.

Appendix 1

See Table 7.

Table 7 Modified parameters for assessing buildings in La Serena, Chile

Parameters and adaption criteria	Class
P1 Façade wall geometry According to original method	**A.** $\frac{H}{B} < 0.40$ **B.** $0.40 \leq \frac{H}{B} < 0.60$ **C.** $0.60 \leq \frac{H}{B} < 1.0$ **D.** $\frac{H}{B} \geq 1.00$
P2 Wall slenderness Slenderness ratio $\lambda = \frac{h}{s}$ - According to NCh 3332: Slenderness ratio should not be greater than 8. According to NTE E.080: Walls with $\lambda \leq 6$ require only a crown beam. Walls with $\lambda > 6$ require both horizontal and vertical reinforcement elements.	**A.** $\lambda \leq 6$ **B.** $6 \leq \lambda \leq 8$ **C.** $8 \leq \lambda \leq 9$ **D.** $\lambda > 9$
P3 Area of wall openings According to original method.	**A.** Opening area less than 20% **B.** Opening area less than 35% **C.** Opening area less than 60% **D.** Opening area greater than 60%
P4 Misalignment of wall opening According to NCh 3332: Maximum opening width should not exceed 2.5 times the thickness. The distance between openings or opening and intersections shall not be less than 3 times the thickness of the wall. According to NTE E.080: Maximum opening width should not exceed 1/3 of the wall length. Distance between opening and intersections shall not be less than 3 nor more than 5 times the thickness of the wall.	**A.** Regular dimensions and aligned in height. **B.** Regular or irregular dimension horizontally misaligned in more than ½ of their height. **C.** Regular or irregular dimension vertically misaligned in more than ½ of their height. Regular or irregular dimension totally misaligned. Relatively large openings (width >1.5 m) at any level of the construction. It is considered that the width should not exceed 1.5 m because the most common wall thickness is 60 cm. **D.** Relatively large openings (width >1.5 m) at any level of the construction + Openings are close to intersections (distance less than 3 times the thickness of the wall).
P5 Interaction between adjacent façade walls Base according to original method. In case the material of adjacent buildings is reinforced concrete or reinforced masonry, the possibility of seismic damage to the earth-based façade increases due to the difference in stiffness.	**A.** In the middle of two façades of the same height. **B.** Contiguous to a façade of the same height and a shorter one. **C.** Contiguous to two shorter façades. **D.** Contiguous to only one, shorter façade. (*) Buildings are downgraded one class if the adjacent building materiality is reinforced masonry or reinforced concrete.

Table 7 (continued)

Parameters and adaption criteria	Class
P6 Masonry quality Materials existing in historic buildings in Chile are incorporated.	**A1.** Stonee masonry with homogeneous units in size and material. **A2.** Brick masonry **B1.** Stone masonry with heterogeneous units in size and material, but well bonded. **B2.** Brick masonry with deficient laying and poor mortar quality. **B3.** Timber framing filled with adobe laid on rowlock stretcher bond or *adobillo*, with a good state of conservation, efficient connections between the elements of timber and no signs of decay by biologic attack or moisture decay. **C1.** Brick masonry with deficient laying and poor mortar quality. **C2.** Timber framing filled with adobe laid on rowlock stretcher bond or *adobillo*, with signs of decay by biologic attack or moisture decay. **C3.** Adobe masonry laid in header bond. **D1.** Adobe masonry laid in stretcher bond.
P7 State of Conservation Moisture is incorporated as a deterioration factor. Moisture accumulation can lead to scour and erosion of materials, which facilitates cracking and decreases the resistance of the structural system (AIS 2004).	**A.** Façade in good condition, with no visible damage. **B.** Façade fissured at the level of coatings, together with points of stress concentration (corners). Presence of repaired cracks. **C.** Façade with signs of settlement (fishbone or sloping cracks); cracks in the middle of the openings (bending), cracking of the cover or by undue load transfer, inclined cracks (by misaligned openings, loading path). **D.** Façade with penetrating fissures and severe disintegration signs; façade walls bulging or out of plumb.
P8 Replacement of the original floors *P*=Percentage of horizontal diaphragms replaced by reinforced concrete structures. According to original method.	**A.** $0 \le P < 25\%$ **B.** $25 \le P < 50\%$ **C.** $50 \le P < 75\%$ **D.** $75 \le P < 100\%$ In the study area only 4% of the buildings assessed have more than 1 level. Buildings with 1 level are considered as Class A.

Table 7 (continued)

	Type of building	Signs of fragility	Class
P9 Connection to orthogonal walls			
According to original method OR architectural typology	Building with poor connections or CO	Yes	D
		No	C
	Presence of strengthening between roof or CL	Yes	C
		No	B
	Presence of strengthening between walls and between walls and roof or CLS	Yes	B
	Rehabilitated	No	A
	(*) UB: Buildings are downgraded if the typology is not clear	–	A
P10 Connection to horizontal diaphragms			
e = Percentage of horizontal diaphragms with efficient connection (%).			
According to original method OR architectural typology	**A.** $e \geq 75\%$	or Rehabilitated buildings and CL/CLS typology in good state of conservation	
	B. $50\% < e < 75\%$	or CL/CLS typology in a regular state of conservation	
	C. $25\% < e < 50\%$	or CO typology in good state of conservation	
	D. $e \leq 25\%$	or CO Typology in a regular or poor state of conservation	
	(*) UB: Buildings are downgraded if the typology is not clear		

Table 7 (continued)

	Impulsive nature	Perimetral straps/beam	Class	State of conserve	
				Poor	Very poor
P11 Impulsive nature of roofing system According to original method	Non impulsive	1 (Yes)	A	B	C
		1–0	A	B	C
		0 (No)	B	C	D
	Slightly impulsive	1 (Yes)	B	C	D
		1–0	B	C	D
		0 (No)	C	D	D
	Impulsive	1 (Yes)	C	D	D
		1–0	C	D	D
		0 (No)	D	–	–

P12 Non-structural elements
Incorporation of non-structural elements of architectural typologies of the historic centre of La Serena

A. No balconies, plaques, ornaments, flower boxes, or other elements (mechanical equipment, air conditioners, signs, etc.)

B. Existence of some lightweight elements (lamps, luminous signs, advertisements, awnings, etc.) attached to the façade. No balconies or parapets

C. Existence of some elements of considerable weight (mechanical equipment, air conditioners etc.) connected to the façade. Presence of concrete coating

D. Existence of balconies, parapets, or other heavy elements attached to the façade

Table 7 (continued)

	Impulsive nature	Perimetral straps/beam	Class	State of conserve	
				Poor	Very poor

P13 Improving elements

According to structural seismic strengthening elements, NCh 3332 states the following:

Structurally compatible materials for raw earth heritage building structures include

Buttresses; Wooden structures (ring beam, wooden keys at the corners); Cane, Steel connectors for timber; Steel or synthetic tensioners on wooden structures; Polypropylene geogrid; Electro-welded mesh

The use of rope mesh has also been proven to improve the seismic performance of one- and two-storey adobe dwellings, thus reducing their inherent high seismic risk (Tarque et al. 2022)

A. There are no external elements

B. Inclusion of wooden ring beam and replacement of adobe spandrel with *quincha* (wattle and daub)

C. Inclusion of seismic strengthening system according to NCh 3332

D. Integral project of structural consolidation according to NCh 3332

Declaration

Conflict of interest The authors report there are no competing interests to declare.

References

Aguado JLP, Ferreira TM, Lourenço PB (2018) The use of a large-scale seismic vulnerability assessment approach for masonry façade walls as an effective tool for evaluating, managing and mitigating seismic risk in historical centers. Int J Archit Herit 12(7–8):1259–1275. https://doi.org/10.1080/15583058.2018.1503366

AIS (2004) Manual para la rehabilitación de viviendas construidas en adobe y tapia pisada. In: Asociación Colombiana de Ingeniería Sísmica (p. 90).

Anglade E, Giatreli AM, Blyth A, Di Napoli B, Parisse F, Namourah Z, Rodrigues H, Ferreira TM (2020) Seismic damage scenarios for the Historic City Center of Leiria, Portugal: analysis of the impact of different seismic retrofitting strategies on emergency planning. Int J Disaster Risk Reduct, 44. https://doi.org/10.1016/j.ijdrr.2019.101432

Aránguiz R, González G, González J, Catalán PA, Cienfuegos R, Yagi Y, Okuwaki R, Urra L, Contreras K, Del Rio I, Rojas C (2016) The 16 September 2015 Chile Tsunami from the Post-Tsunami Survey and numerical modeling perspectives. Pure Appl Geophys 173(2):333–348. https://doi.org/10.1007/s00024-015-1225-4

Arriagada Luco C, Jeri T (2021) Revitalización de barrios patrimoniales en áreas metropolitanas: propuestas de monitoreo y gestión integrada. Estoa 11(21):103–116. https://doi.org/10.18537/est.v011.n021.a09

Baquedano Juliá P, Ferreira TM (2021) From single- to multi-hazard vulnerability and risk in Historic Urban Areas: a literature review. In: Natural Hazards (Issue 0123456789). Springer, Netherlands. https://doi.org/10.1007/s11069-021-04734-5

Barrientos SE (2010) Terremoto (M=8.8) del 27 de febrero de 2010 en Chile. Revista de La Asociación Geológica Argentina 67(3):412–420.

Benedetti D, Petrini V (1984) On seismic vulnerability of masonry buildings: proposal of an evaluation procedure. L'industria Delle Construzioni 18:66–78

Bernardini A, Giovinazzi S, Lagomarsino S, Parodi S (2007) Vulnerabilità e previsione di danno a scala territoriale secondo una metodologia macrosismica coerente con la scala EMS-98. ANIDIS, XII Convegno Nazionale l'ingegneria Sismica in Italia, 10 a 14 Giugno, Pisa, November 2015. http://ir.cante rbury.ac.nz/handle/10092/4060

Birkmann J (2006). Measuring vulnerability to promote disaster-resilient societies and to enhance adaptation: Conceptual frameworks and definitions. In: Birkmann J (ed) Measuring vulnerability to natural hazards; towards disaster resilient societies, 1st edn, Vol. 01, pp. 9–54. United Nations University Press, Tokyo. https://doi.org/10.1111/j.1539-6975.2010.01389.x

Birkmann J (2013) Part I Basic principles and theoretical basis. Measuring vulnerability to promote disaster-resilient societies and to enhance adaptation: Discussion of conceptual frameworks and definitions. In: Birkmann J (ed) Measuring vulnerability to natural hazards: Towards disaster resilient societies, 2nd edn, pp. 9–79. United Nations University Press, Tokyo.

Birkmann J, Cardona OD, Carreño ML, Barbat AH, Pelling M, Schneiderbauer S, Kienberger S, Keiler M, Alexander D, Zeil P, Welle T (2013) Framing vulnerability, risk and societal responses: the MOVE framework. Nat Hazards 67(2):193–211. https://doi.org/10.1007/s11069-013-0558-5

Bohle H-G (2001) Vulnerability and Criticality: Perspectives from Social Geography. IHDP Update 2(01):3–5

Bosher L, Kim D, Okubo T, Chmutina K, Jigyasu R (2019) Dealing with multiple hazards and threats on cultural heritage sites: an assessment of 80 case studies. Disaster Prevent Manag Int J 29(1):109–128. https://doi.org/10.1108/DPM-08-2018-0245

Bramerini F, Di Pasquale G, Orsini A, Pugliese A, Romeo R, Sabetta F (1995) Rischio sismico del territorio italiano. Proposta per una metodologia e risultati preliminari. Rapporto tecnico del Servizio Sismico SSN (in Italian).

Bronfman NC, Repetto PB, Guerrero N, Castañeda JV (2021) Temporal evolution in social vulnerability to natural hazards. Nat Hazards 107(2):1757–1784. https://doi.org/10.1007/s11069-021-04657-1

Bruquetas Callejo M, Moreno Fuentes FJ, Walliser Martínez A (2005) La regeneración de barrios desfavorecidos. In Fundación Alternativas. Fundación Alternativas. Proyecto UGIS (Urban Governance, Social Inclusión and Sustainability) desarrollado, V Programa Marco de Investigación de la Comisión Europea. https://www.fundacionalternativas.org/laboratorio/documentos/documentos-de-trabajo/la-regeneracion-de-barrios-desfavorecidos

Calvi GM, Pinho R, Magenes G, Bommer JJ, Restrepo-Vélez LF, Crowley H (2006) Development of seismic vulnerability assessment methodologies over the past 30 years. ISET J Earthq Technol 43(3):75–104

Candia G, de Pascale GP, Montalva G, Ledezma C (2017) Geotechnical Aspects of the 2015 M w 8.3 Illapel Megathrust Earthquake Sequence in Chile. EarthqSpectra 33(2):709–728. https://doi.org/10.1193/031716EQS043M

Cardona OD (2003) The need for rethinking the concepts of vulnerability and risk from a holistic perspective: a necessary review and criticism for effective. In: Bankoff G, Frerks G (eds) Mapping vulnerability: disasters, develpment and people. (D. Hilhors). Earthscan Publishers, Routledge.

Carreño ML, Cardona OD, Barbat AH (2007) Urban seismic risk evaluation: a holistic approach. Nat Hazards 40(1):137–172. https://doi.org/10.1007/s11069-006-0008-8

Carrión F (2001) Centros Históricos de America Latina y el Caribe. In UNESCO-BID, Ministerio de Cultura y Comunicación de Francia, FLACSO , Quito, Ecuador.

CEPAL (2016) La matriz de la desigualdad social en América Latina. I Reunión de La Mesa Directiva de La Conferencia Regional Sobre Desarrollo Social de América Latina y El Caribe.

CEPAL (2022) Panorama Social de América Latina y el Caribe (LC/PUB.2022/15-P). https://www.cepal.org/es/publicaciones/48518-panorama-social-america-latina-caribe-2022-la-transformacion-la-educacion-como

Chieffo N, Formisano A, Landolfo R, Milani G (2022) A vulnerability index based-approach for the historical centre of the city of Latronico (Potenza, Southern Italy). Eng Failure Anal 136(January):106207. https://doi.org/10.1016/j.engfailanal.2022.106207

Cisternas ME (2011) Responsabilidad social de los geocientistas en el manejo de riesgos: Enseñanzas derivadas de la experiencia chilena con el megaterremoto del 27 de febrero 2010. GOAL 2011: Geo-Risk Management a German-Latin American Approach, pp 19–24.

CMN (2010) Elaboración del Instructivo de Intervención Zona Típica o Pintoresca "Centro Histórico de La Serena." Realiza Gestión de Patrimonio Ltda.

CNDU (2017) Propuestas para un modelo integral de conservación del patrimonio urbano, Consejo Nacional de Desarrollo Urbano.

CNDU (2019) Sistema de indicadores y estándares de calidad de vida y desarrollo urbano, Consejo Nacional de Desarrollo Urbano.

CNDU (2021) Propuestas para la regeneración urbana de las ciudades chilenas Consejo Nacional de Desarrollo Urbano.

Contreras M, Winckler P (2013) Pérdidas de vidas, viviendas, infraestructura y embarcaciones por el tsunami del 27 de Febrero de 2010 en la costa central de Chile. Obras y Proyectos 14:6–19. http://www.scielo.cl/scielo.php?script=sci_arttext&pid=S0718-28132013000200001

Contreras Vergara D (2018) Casa Jiliberto. Evolución de la tipología arquitectónica residencial en La Serena desde la época colonial hasta fines del siglo XIX. Universidad de Chile.

CSN (2013) Informe Técnico: Sismicidad y terremotos en Chile. In Centro Sismológico Nacional. Universidad de Chile. https://www.csn.uchile.cl/archivo/informes-tecnicos/

CSN (2016) Artículo de Prensa: Avances en la zonificación sísmica de Chile. Centro Sismológico Nacional. Universidad de Chile. https://www.csn.uchile.cl/avances-en-la-zonificacion-sismica-de-chile/

Cutter SL, Boruff BJ, Shirley WL (2003) Social vulnerability to environmental hazards. Soc Sci Q 84(2):242–261. https://doi.org/10.1111/1540-6237.8402002

DA-MOP (2000) Inventario del Patrimonio Cultural Inmueble de Chile.

de Araujo Pinheiro M (2020) Women, vulnerability, resilience and natural disasters: interview with Marta de Araujo Pinheiro. https://hal-sciencespo.archives-ouvertes.fr/hal-03392009

Decree No. 499 (1981) Declara Monumentos Históricos y Zona Típica, el área de la ciudad tradicional de La Serena. Consejo de Monumentos Nacionales.

Farías Vega C (2019) Columna de sismología: El potente terremoto de Coquimbo, su cronología, y por qué se sintió tan fuerte. Diario La Tercera. https://web.archive.org/web/20200227195557/https://www.latercera.com/tendencias/noticia/columna-sismologia-potente-terremoto-coquimbo-cronologia-se-sintio-tan-fuerte/495506/?outputType=amp

Federal Emergency Management Agency (FEMA) (1999) Induced Damage Models - Fire Following Earthquake. In: HAZUS-MH MR4 Technical Manual. FEMA. www.fema.gov/plan/prevent/hazus.

Fernández J, Pastén C, Ruiz S, Leyton F (2019) Damage assessment of the 2015 Mw 8.3 Illapel earthquake in the North-Central Chile. Nat Hazards 96(1):269–283. https://doi.org/10.1007/s11069-018-3541-3

Ferreira TM, Maio R, Costa AA, Vicente R (2017a) Seismic vulnerability assessment of stone masonry façade walls: calibration using fragility-based results and observed damage. Soil Dyn Earthq Eng 103:21–37. https://doi.org/10.1016/j.soildyn.2017.09.006

Ferreira TM, Maio R, Vicente R (2017b) Analysis of the impact of large scale seismic retrofitting strategies through the application of a vulnerability-based approach on traditional masonry buildings. Earthq Eng Eng Vib 16(2):329–348. https://doi.org/10.1007/s11803-017-0385-x

Ferreira TM, Maio R, Vicente R (2017c) Seismic vulnerability assessment of the old city centre of Horta, Azores: calibration and application of a seismic vulnerability index method. Bull Earthq Eng 15(7):2879–2899. https://doi.org/10.1007/s10518-016-0071-9

Ferreira TM, Mendes N, Silva R (2019) Multiscale seismic vulnerability assessment and retrofit of existing masonry buildings. Buildings 9(4). https://doi.org/10.3390/buildings9040091

Ferreira TM, Vicente R, Mendes da Silva JAR, Varum H, Costa A (2013) Seismic vulnerability assessment of historical urban centres: Case study of the old city centre in Seixal, Portugal. Bull Earthq Eng 11(5):1753–1773. https://doi.org/10.1007/s10518-013-9447-2

Ferreira TM, Vicente R, Varum H (2014) Seismic vulnerability assessment of masonry facade walls: development, application and validation of a new scoring method. Struct Eng Mech 50(4):541–561. https://doi.org/10.12989/sem.2014.50.4.541

Flanagan BE, Gregory EW, Hallisey EJ, Heitgerd JL, Lewis B (2011) A Social Vulnerability Index for Disaster Management. J Homeland Security Emerg Manag 8(1). https://doi.org/10.2202/1547-7355.1792

Fordham MH (1998) Making women visible in disasters: problematising the private domain. Disasters 22(2):126–143. https://doi.org/10.1111/1467-7717.00081

Formisano A, Florio G, Landolfo R, Mazzolani FM (2015) Numerical calibration of an easy method for seismic behaviour assessment on large scale of masonry building aggregates. Adv Eng Softw 80(C):116–138. https://doi.org/10.1016/j.advengsoft.2014.09.013

GeoBytesGCSE (2007) Bam 2003. Case Study of an Earthquake in an LEDC. https://geobytesgcse.blogspot.com/2007/01/case-study-of-earthquake-in-ledc-bam.html

Giovinazzi S, Lagomarsino S (2004) A macroseismic method for the vulnerability assessment of buildings. In: 13th World Conference on Earthquake Engineering, p. 896.

Goodman ZT, Stamatis CA, Stoler J, Emrich CT, Llabre MM (2021) Methodological challenges to confirmatory latent variable models of social vulnerability. Nat Hazards 106(3):2731–2749. https://doi.org/10.1007/s11069-021-04563-6

Grünthal G (1998) Cahiers du Centre Européen de Géodynamique et de Séismologie: European Macroseismic Scale. 15.

Hufschmidt G (2015) A comparative analysis of several vulnerability concepts. August 2011. https://doi.org/10.1007/s11069-011-9823-7

IMTA (2015) Atlas de vulnerabilidad hídrica en México ante el cambio climático (Instituto Mexicano de Tecnología del Agua (ed.)).

INE (2017) íntesis Resultados Censo 2017. Instituto Nacional de Estadísticas, Santiago.

NCh 433 .Of 72 - Cálculo antisísmico de edificios (Earthquake resistant design of buildings) (1996).

NCh 3332 (2013) Estructuras - Intervención de construcciones patrimoniales de tierra cruda - Requisitos del proyecto estructural (Structural design - Retrofitting of historic earth buildings - Requirements for the structural design planning), Instituto Nacional De Normalización

Izquierdo-Horna L, Kahhat R (2020) An interdisciplinary approach to identify zones vulnerable to earthquakes. Int J Disaster Risk Reduct 48(March):101592. https://doi.org/10.1016/j.ijdrr.2020.101592

Jiménez B, Pelà L, Hurtado M (2018) Building survey forms for heterogeneous urban areas in seismically hazardous zones. Application to the historical center of Valparaíso, Chile. Int J Architectural Herit 12(7–8):1076–1111. https://doi.org/10.1080/15583058.2018.1503370

Juntunen L (2006) Addressing social vulnerability to hazards. Disaster Safety Rev 4(2):3–10

Kanno E, Torres C (2020) Conservación preventiva en edificios patrimoniales de estructura mixta en el centro histórico de La Serena: Propuesta de soluciones a partir de un análisis de las tipologías y sus patrones deterioro. Universidad de Chile.

Kaztman R, Filgueira C (1999) Marco conceptual sobre activos, vulnerabilidad y estructura de oportunidades. NU. CEPAL. https://www.cepal.org/es/publicaciones/28663-marco-conceptual-activos-vulnerabilidad-estructuras-oportunidades

Maio R, Ferreira TM, Vicente R (2018) A critical discussion on the earthquake risk mitigation of urban cultural heritage assets. Int J Disaster Risk Reduct 27(October):239–247. https://doi.org/10.1016/j.ijdrr.2017.10.010

Marquéz de la Plata R (1979) Patrimonio Cultural de Coquimbo y La Serena. Ministerio de Vivienda y Urbanismo.

Mengal A, Goda K, Ashraf M, Murtaza G (2021) Social vulnerability to seismic-tsunami hazards in district Gwadar, Balochistan, Pakistan. Nat Hazards 108(1):1159–1181. https://doi.org/10.1007/s11069-021-04724-7

MIDESO/PNUD (2021) Evolución de la pobreza 1990–2017: ¿Como ha cambiado Chile?, Subsecretaria de Evaluación Social Ministerio de Desarrollo Social Chile, Programa de Naciones Unidas para el Desarrollo, Santiago de Chile.

Misseri G, Palazzi C, Rovero L (2020) Seismic vulnerability of timber-reinforced earthen structures through standard and non–standard limit analysis. Eng Struct 215(February):110663. https://doi.org/10.1016/j.engstruct.2020.110663

Musson RMW, Grünthal G, Stucchi M (2010) The comparison of macroseismic intensity scales. J Seismolog 14(2):413–428. https://doi.org/10.1007/s10950-009-9172-0

MVM (1973) El Orden que se ha de Thener en Descubrir y Poblar, transcripción de las Ordenanzas de descubrimiento, nuevo población y pacificación de las Indias dadas por Felipe II, el 13 de julio de 1573, en el Bosque de Segovia, Archivo General de Indias de Sevilla. In: Ministerio de la Vivienda.

Neves F, Costa A, Vicente R, Oliveira CS, Varum H (2012) Seismic vulnerability assessment and characterisation of the buildings on Faial Island, Azores. Bull Earthq Eng 10(1):27–44. https://doi.org/10.1007/s10518-011-9276-0

ONU-CEPAL (2001) Informe de la Reunión de expertos: Seminario Internacional sobre las diferentes expresiones de la vulnerabilidad social en América Latina y el Caribe. División de Población de La Comisión Económica Para América Latina y El Caribe (CEPAL) - Centro Latinoamericano y Caribeño de Demografía (CELADE).

Ortega J, Vasconcelos G, Rodrigues H, Correia M, Lourenço PB (2017) Traditional earthquake resistant techniques for vernacular architecture and local seismic cultures: a literature review. J Cult Herit 27:181–196. https://doi.org/10.1016/j.culher.2017.02.015

Palazzi NC, Misseri G, Rovero L, de La Llera JC (2021) Seismic vulnerability assessment of a 17 th century colonial adobe church in the central valley of Chile. In: 12th International conference on structural analysis of historical constructions.

Palazzi NC, Barrientos M, Sandoval C, De JC (2022) Seismic Vulnerability Assessment of the Yungay ' s Historic Urban Center in Santiago, Chile Seismic Vulnerability Assessment of the Yungay ' s Historic Urban. J Earthquake Eng 00(00):1–28. https://doi.org/10.1080/13632469.2022.2087793

Pardo M, Comte D, Monfret T, Boroschek R, Astroza M (2002) The October 15, 1997 Punitaqui earthquake (Mw=7.1): A destructive event within the subducting Nazca plate in the Central Chile. Tectonophysics 345(1–4):199–210. https://doi.org/10.1016/S0040-1951(01)00213-X

Park G, Xu Z (2022) The constituent components and local indicator variables of social vulnerability index. Nat Hazards 110(1):95–120. https://doi.org/10.1007/s11069-021-04938-9

Pulido L (2000) Rethinking environmental racism: White privilege and urban development in southern California. Ann Assoc Am Geogr 90(1):12–40. https://doi.org/10.1111/0004-5608.00182

Ramírez Eudave R, Ferreira TM, Vicente R (2022) Parameter-based seismic vulnerability assessment of Mexican historical buildings: Insights, suitability, and uncertainty treatment. Int J Disaster Risk Reduct 74(November 2021):102909. https://doi.org/10.1016/j.ijdrr.2022.102909

Robat Mili R, Amini Hosseini K, Izadkhah YO (2018) Developing a holistic model for earthquake risk assessment and disaster management interventions in urban fabrics. Int J Disaster Risk Reduct 27(October 2017):355–365. https://doi.org/10.1016/j.ijdrr.2017.10.022

Rojas E (2004) Volver al centro: La recuperación de áreas urbanas centrales. Banco Interamericano de Desarrollo - Departamento de Desarrollo Sostenible.

Ruiz S, Madariaga R (2018) Historical and recent large megathrust earthquakes in Chile. Tectonophysics 733:37–56. https://doi.org/10.1016/j.tecto.2018.01.015

Ruiz S, Ammirati J, Leyton F, Cabrera L, Potin B, Madariaga R (2019) The January 2019 (Mw 6.7) Coquimbo Earthquake: insights from a seismic sequence within the Nazca Plate. Seismol Res Lett. https://doi.org/10.1785/0220190079

Sánchez-González D, Egea-Jiménez C (2011) Enfoque de vulnerabilidad social para investigar las desventajas socioambientales: Su aplicación en el estudio de los adultos mayores. Papeles de Población 17(69)151–185. http://www.scielo.org.mx/scielo.php?script=sci_arttext&pid=S1405-74252011000300006&lng=es&nrm=iso&tlng=es

Scheuer S, Haase D, Meyer V (2011) Exploring multicriteria flood vulnerability by integrating economic, social and ecological dimensions of flood risk and coping capacity: from a starting point view towards an end point view of vulnerability. Nat Hazards 58(2):731–751. https://doi.org/10.1007/s11069-010-9666-7

NTE.080 (2017) Reglamento Nacional de Edificaciones del Peru (National Building Regulations of Peru). Ministerio de Vivienda, Construcción y Saneamiento, 1, 24. Servicio Nacional de Capacitación para la Industria de la Construcción—SENCICO (National Training Service for the Construction, & Industry)

Shapira S, Novack L, Bar-Dayan Y, Aharonson-Daniel L (2016) An integrated and interdisciplinary model for predicting the risk of injury and death in future earthquakes. PLoS ONE 11(3):1–11. https://doi.org/10.1371/journal.pone.0151111

Spielman SE, Tuccillo J, Folch DC, Schweikert A, Davies R, Wood N, Tate E (2020) Evaluating social vulnerability indicators: criteria and their application to the Social Vulnerability Index. Nat Hazards 100(1):417–436. https://doi.org/10.1007/s11069-019-03820-z

Tarque N, Blondet M, Vargas-Neumann J, Yallico-Luque R (2022) Rope mesh as a seismic reinforcement for two-storey adobe buildings. Bull Earthq Eng 20(8):3863–3888. https://doi.org/10.1007/s10518-022-01346-7

Tate E (2012) Social vulnerability indices: a comparative assessment using uncertainty and sensitivity analysis. Nat Hazards 63(2):325–347. https://doi.org/10.1007/s11069-012-0152-2

Tolles EL, Kimbro EE, Ginell WS (2002) Planning and engineering guidelines for the seismic retrofitting of historic adobe structures retrofitting of historic adobe structures. Getty Publications, Chennai

Turner B, Kasperson RE, Matson PA, Mccarthy JJ, Corell RW, Christensen L, Eckley N, Kasperson JX, Luers A, Martello ML, Polsky C, Pulsipher A, Schiller A (2003) A framework for vulnerability analysis in sustainability science. Proc Natl Acad Sci 100(14). https://doi.org/10.1073/pnas.1231335100

UN (2005) Hyogo framework for action 2005–2015: building the resilience of Nations and Communities to Disasters.

UN (2015) Sendai framework for disaster risk reduction 2015–2030.

UNISDR (2009) Disaster. In: UNISDR Terminology on Disaster Risk Reduction (Vol. 1, p. 35). United Nations. https://doi.org/10.1021/cen-v064n005.p003

Vicente R, Parodi S, Lagomarsino S, Varum H, Silva JARM (2011) Seismic vulnerability and risk assessment: case study of the historic city centre of Coimbra, Portugal. Bull Earthq Eng 9(4):1067–1096. https://doi.org/10.1007/s10518-010-9233-3

Villarreal M, Meyer MA (2020) Women's experiences across disasters: a study of two towns in Texas, United States. Disasters 44(2):285–306. https://doi.org/10.1111/disa.12375

Wisner B, Blaikie P, Cannon T, Davis I (2004) At risk: natural hazards, People's vulnerability and disasters. Routledge

Wood NJ, Burton CG, Cutter SL (2010) Community variations in social vulnerability to Cascadia-related tsunamis in the U.S. Pacific Northwest. Nat Hazards 52(2):369–389. https://doi.org/10.1007/s11069-009-9376-1

Authors and Affiliations

Pilar Baquedano-Juliá[1] ⬤ **· Tiago Miguel Ferreira[2] · Camilo Arriagada-Luco[3] · Cristián Sandoval[4] · Nuria Chiara Palazzi[5,6,7] · Daniel V. Oliveira[1]**

✉ Pilar Baquedano-Juliá
   id8020@alunos.uminho.pt

[1] Department of Civil Engineering, ISISE, University of Minho, Guimarães, Portugal

[2] College of Arts, Technology and Environment, School of Engineering, University of the West of England (UWE Bristol), Bristol, UK

[3] Department of Urban Planning, Faculty of Architecture and Urbanism, Universidad de Chile, Santiago, Chile

[4] Department of Structural and Geotechnical Engineering, Pontificia Universidad Católica de Chile, Santiago, Chile

[5] Faculty of Architecture, Design and Urban Studies, Pontificia Universidad Católica de Chile, Santiago, Chile

[6] National Research Center for Integrated Natural Disaster Management (CIDIGEN), ANID/FONDAP/15110017, Santiago, Chile

[7] Centro del Patrimonio Cultural UC, Santiago, Chile